Effect of flow damping on drift-tearing magnetic islands in tokamak plasmas

R. Fitzpatrick and F. L. Waelbroeck
Department of Physics, Institute for Fusion Studies, University of Texas at Austin, Austin, Texas 78712, USA

(Received 8 April 2009; accepted 9 July 2009; published online 28 July 2009)

A systematic fluid theory of nonlinear drift-tearing magnetic island dynamics in a conventional large aspect-ratio low-β circular cross-section tokamak plasma is derived from a set of single-helicity reduced neoclassical-magnetohydrodynamical equations which incorporate electron and ion diamagnetic flows, ion gyroviscosity, poloidal and toroidal flow damping, cross flux-surface momentum and particle transport, the sound wave, and the drift wave. The equations neglect the compressible Alfvén wave, electron inertia, the electron viscosity tensor, magnetic field-line curvature, and finite ion orbit widths. A collisional closure is used for plasma dynamics parallel to the magnetic field. The influence of various different levels of flow damping on the phase velocity of an isolated island, as well as the ion polarization term appearing in its Rutherford equation, are investigated in detail. Furthermore, it is found that, under certain circumstances, a locked island is subject to destabilizing ion polarization term to which a comparable isolated (i.e., rotating) island is not. © *2009 American Institute of Physics*. [DOI: 10.1063/1.3191719]

I. INTRODUCTION

A tokamak is a device which is designed to trap a thermonuclear plasma on a set of toroidally nested magnetic flux surfaces.[1] Heat and particles are able to *flow around* the flux surfaces relatively rapidly due to the free streaming of charged particles along magnetic field lines. On the other hand, heat and particles are only able to *diffuse across* the flux surfaces relatively slowly, assuming that the magnetic field strength is large enough to ensure that the particle gyroradii are much smaller than the minor radius of the device.[2]

Tokamak plasmas are subject to a number of macroscopic instabilities which limit their effectiveness.[3] Such instabilities can be divided into two broad classes. So-called *ideal instabilities* are nonreconnecting modes which disrupt the plasma in a matter of microseconds. However, such instabilities can easily be avoided by limiting the plasma pressure and tailoring the equilibrium density and temperature profiles.[4] *Tearing modes*, on the other hand, are relatively slowly growing instabilities which are far more difficult to avoid.[4,5] These instabilities tend to saturate at relatively low levels[6–8] in the process reconnecting magnetic flux surfaces to form helical structures known as *magnetic islands*. Magnetic islands are radially localized structures centered on the so-called *rational flux surfaces*, which satisfy $\mathbf{k}\cdot\mathbf{B}=0$, where $\mathbf{k}$ is the wavenumber of the instability and $\mathbf{B}$ is the equilibrium magnetic field. Islands degrade plasma confinement because they enable heat and particles to flow very rapidly along field lines from their inner to their outer radii, implying an almost complete loss of confinement in the region lying between these radii.[9]

The aim of this paper is to continue the development of a systematic drift- magnetohydrodynamical (MHD) fluid theory of magnetic island dynamics in a conventional large aspect-ratio low-β circular cross-section tokamak plasma by generalizing the theory introduced in Ref. 10 to take *poloidal and toroidal flow damping* into account. Such damping is inevitably generated from the interaction of the parallel ion viscosity tensor with the variations in the magnetic field strength around tokamak flux surfaces which are driven by toroidicity and nonaxisymmetric error fields[11,12] and is generally thought to play an important role in island dynamics.[13]

In this paper, for the sake of simplicity, we shall employ a *single-helicity approximation* to model the island geometry and thereby reduce the problem to an essentially two dimensional one. We shall also employ a *collisional closure* for the plasma dynamics parallel to the magnetic field.

II. REDUCED NEOCLASSICAL MHD MODEL

A. Coordinates

Consider a large aspect-ratio low-β circular cross-section tokamak plasma equilibrium. Let us adopt the standard toroidal coordinates (r,θ,φ), where r is the magnetic flux-surface minor radius, θ is the poloidal angle, and φ is the toroidal angle. Of course, r is a flux-surface label. In the following, $\mathbf{e}_\theta$ denotes a unit vector pointing in the θ-direction, etc.

B. Asymptotic matching

Consider a radially localized magnetic island, formed as the saturated state of a nonlinear tearing instability, which is embedded in the aforementioned plasma equilibrium. The plasma is conveniently divided into an "inner region," which comprises the plasma in the immediate vicinity of the island, and an "outer region," which comprises the remainder of the plasma. As is well known, standard linear ideal-MHD analysis is perfectly adequate in the outer region, whereas nonlinear nonideal drift-MHD analysis is generally required in the inner region. Let us assume that a conventional linear ideal-

MHD solution has been found in the outer region. Such a solution is characterized by a single parameter Δ' known as the *tearing stability index*, which is defined as the jump in the logarithmic derivative of the radial component of the perturbed magnetic field across the inner region.[5] In general, if the island interacts electromagnetically with an external structure, such as a resistive wall or a resonant error field, then Δ' is *complex*. The *real part* of the tearing stability index measures the *free energy* available, either in the outer region or the region external to the plasma, to drive the growth of the magnetic island.[14] The island is destabilized if $\mathrm{Re}(\Delta')>0$. The *imaginary part* of the tearing stability index measures the net *electromagnetic locking force* exerted on the island region by any external structures.[14] It remains to obtain a nonlinear nonideal drift-MHD solution in the inner region and then to asymptotically match this solution to the aforementioned linear ideal-MHD solution at the boundary between the inner and the outer regions.

C. Drift-MHD model

In the inner region, our starting point is the following drift-MHD model of the plasma dynamics, which is adapted from Ref. 15,

$$\mathbf{E}+\mathbf{V}\times\mathbf{B}+\frac{1}{en_0}\left[\nabla P-\frac{\tau}{1+\tau}(\mathbf{b}\cdot\nabla P)\mathbf{b}-\mathbf{J}\times\mathbf{B}\right]=\eta(\mathbf{J}-J_0\mathbf{b}), \tag{1}$$

$$m_i n_0\left[\left(\frac{\partial}{\partial t}+\mathbf{V}\cdot\nabla+\frac{\tau}{1+\tau}\mathbf{V}_*\cdot\nabla\right)\mathbf{V}-\frac{\tau}{1+\tau}\mathbf{V}_*\cdot\nabla([\mathbf{b}\cdot\mathbf{V}]\mathbf{b})\right]=\mathbf{J}\times\mathbf{B}-\nabla P-m_i n_0\nu_\theta(\mathbf{V}_i\cdot\mathbf{e}_\theta-V_{\theta i}^{\mathrm{nc}})\mathbf{e}_\theta-m_i n_0\nu_\varphi(\mathbf{V}_i\cdot\mathbf{e}_\varphi-V_{\varphi i}^{\mathrm{nc}})\mathbf{e}_\varphi+\mu\nabla^2\mathbf{V}_i, \tag{2}$$

$$\left(\frac{\partial}{\partial t}+\mathbf{V}\cdot\nabla\right)P+\Gamma P\,\nabla\cdot\mathbf{V}=\kappa\nabla^2 P. \tag{3}$$

Here, $\mathbf{b}=\mathbf{B}/B$, $\mathbf{V}_*=\mathbf{b}\times\nabla P/(en_0B)$, and $\mathbf{V}_i=\mathbf{V}+\tau(1+\tau)^{-1}\mathbf{V}_*$. The model is completed by Maxwell's equations: $\nabla\cdot\mathbf{B}=0$, $\nabla\times\mathbf{E}=-\partial\mathbf{B}/\partial t$, and $\nabla\times\mathbf{B}=\mu_0\mathbf{J}$. In the above, $\mathbf{E}$ is the electric field, $\mathbf{B}$ is the magnetic field, $\mathbf{J}$ is the electric current density, $\mathbf{V}$ is the guiding center velocity, $\mathbf{V}_*$ is the diamagnetic velocity, $\mathbf{V}_i$ is the ion fluid velocity, P is the total pressure, e is the magnitude of the electron charge, $Z=1$ is the ion charge number, m_i is the ion mass, n_0 is the (constant) background electron number density, τ is the (constant) ratio of the ion to the electron temperature, $\Gamma=5/3$ is the ratio of specific heats, η is the plasma resistivity, and J_0 is the (constant) equilibrium parallel current density. The above equations incorporate ion and electron diamagnetic flows (including the contribution of ion gyroviscosity[15]) but neglect electron inertia, the electron viscosity tensor, and magnetic field-line curvature. The neglect of the electron viscosity tensor, which is justified provided the plasma is sufficiently collisional, also implies the neglect of the bootstrap current.[11] Field-line curvature is neglected because it cannot be dealt with within the context of a single-helicity model.[16,17] The plasma equation of motion (2) includes a phenomenological ion viscosity term, with the associated viscosity coefficient μ, which is supposed to mimic momentum transport due to small-scale turbulence. This equation also contains phenomenological poloidal and toroidal flow damping terms, with the associated damping rates ν_θ and ν_φ, respectively. These terms act to relax the poloidal and toroidal components of the ion fluid velocity toward the (constant) values $V_{\theta i}^{\mathrm{nc}}$ and $V_{\varphi i}^{\mathrm{nc}}$, respectively. As is well known, the poloidal flow damping term originates from the interaction of the parallel ion viscosity tensor with the naturally occurring poloidal variations in the magnetic field-strength around flux surfaces.[11] On the other hand, the toroidal flow damping term originates from the interaction of the parallel ion viscosity tensor with any toroidal variations in the magnetic field strength around flux surfaces induced, for instance, by nonaxisymmetric error fields.[12] Both of our phenomenological flow damping terms are greatly simplified in structure and can be thought of as the *flux-surface averages* of the true damping terms.[18] Furthermore, the neoclassical ion poloidal and toroidal velocities, $V_{\theta i}^{\mathrm{nc}}$ and $V_{\varphi i}^{\mathrm{nc}}$, are both fully specified by standard neoclassical theory.[12,19–21] Finally, the pressure equation (3) contains a phenomenological diffusion term, with the associated diffusivity κ, which is supposed to mimic energy transport due to small-scale turbulence.

D. Single-helicity approximation

The inner region is radially localized in the vicinity of the m_θ, n_φ mode rational surface, minor radius r_s. Here, m_θ and n_φ are the respective poloidal and toroidal mode numbers of the magnetic island. The equilibrium magnetic field at the rational surface is written as $\mathbf{B}_0=B_0(0,\epsilon/q,1)$, where $\epsilon=r_s/R_0\ll 1$, $q=m_\theta/n_\varphi$, and R_0 is the plasma major radius. All variables are assumed to be functions of $x=r-r_s$ and

$$\zeta=m_\theta\theta-n_\varphi\varphi-\omega t \tag{4}$$

only. Here, ω is the island frequency in the laboratory frame. The magnetic field, electric field and guiding center velocity can be written in the forms

$$\mathbf{B}=\nabla A_\parallel\times\mathbf{n}+B_\parallel\mathbf{n}, \tag{5}$$

$$\mathbf{E}=-\nabla\Phi-\frac{\partial A_\parallel}{\partial t}\mathbf{n}, \tag{6}$$

$$\mathbf{V}\simeq-\frac{\nabla\Phi\times\mathbf{n}}{B_0}+V_\parallel\mathbf{n}, \tag{7}$$

respectively, where $\mathbf{n}=(0,\epsilon/q,1)$ is a unit [to $\mathcal{O}(\epsilon/q)$] vector parallel to the local equilibrium magnetic field at the rational surface and

$$B_\parallel\simeq B_0-\frac{\mu_0\delta P}{B_0}, \tag{8}$$

$$\delta P = (1+\tau)T_e \delta n = P - P_0. \tag{9}$$

In addition, $B_0 \gg \mu_0 \delta P / B_0$ and $P_0 = (1+\tau)T_e n_0 \gg \delta P$ are spatial constants, T_e is the (constant) background electron temperature, and δn is the perturbed electron number density. It is helpful to define the unit [to $\mathcal{O}(\epsilon/q)$] wavevector $\mathbf{k} = (0,1,-\epsilon/q)$ at the rational surface, where $\mathbf{k} \propto \nabla\zeta$ and $\mathbf{k}\cdot\mathbf{n} = 0$.

E. Reduced neoclassical-MHD equations

Following the procedure set out in Ref. 22, we can eliminate the compressional Alfvén wave from Eqs. (1)–(3) to obtain the following set of (normalized) reduced neoclassical-MHD equations:

$$0 = [\phi - n, \psi] + \delta_e \hat{\eta} J, \tag{10}$$

$$0 = [\phi, n] + [V + \rho^2 J, \psi] + D\partial_X^2 n, \tag{11}$$

$$0 = [\phi, \partial_X^2 \phi] - \frac{\tau}{2}\{\partial_X^2[\phi,n] + [\partial_X^2\phi, n] + [\partial_X^2 n, \phi]\} + [J,\psi] + \hat{\nu}_\theta \partial_X\{\xi V - \partial_X(\phi + \tau n)\} - \hat{\nu}_\varphi \xi \partial_X V + \hat{\mu}\partial_X^4(\phi + \tau n), \tag{12}$$

$$0 = [\phi, V] + \alpha^2[n,\psi] - \hat{\nu}_\theta(\epsilon/q)^2\xi^{-1} \times\{\xi V - \partial_X(\phi + \tau n) + \hat{V}_p - \hat{V}_{\rm nc}\} - \hat{\nu}_\varphi V + \hat{\mu}\partial_X^2 V, \tag{13}$$

plus

$$\partial_X^2 \psi = -1 + \delta_e J. \tag{14}$$

Moreover, $\partial_X \equiv \partial/\partial X$ and

$$[A,B] \equiv \frac{\partial A}{\partial X}\frac{\partial B}{\partial \zeta} - \frac{\partial A}{\partial \zeta}\frac{\partial B}{\partial X}. \tag{15}$$

In addition, $X = x/w$, $\psi = (L_s/B_0 w^2)A_\parallel$, $J = (L_s/B_0\delta_e)(\mu_0 J_0 + \nabla^2 A_\parallel)$, $\phi = (-\Phi/wV_{*e}B_0) + V_p X$, $V_{*e} = T_e/(eB_0 L_n)$, $\hat{V}_p = V_p/V_{*e}$, $V_p = \omega/k_\theta$, $k_\theta = m_\theta/r_s$, $n = -(L_n/w)\delta n/n_0$, $V = (\Gamma L_n/L_s)(V_\parallel - V_{\varphi i}^{\rm nc})/V_{*e}$, $\hat{\eta} = \eta/(\mu_0 k_\theta V_{*e} w^2)$, $\hat{\mu} = \mu/(n_0 m_i k_\theta V_{*e} w^2)$, $\hat{\nu}_{\theta,\varphi} = \nu_{\theta,\varphi}/(k_\theta V_{*e})$, $D = \hat{\kappa} + (1+\tau)\beta_e\hat{\eta}$, $\hat{\kappa} = \kappa/(k_\theta V_{*e} w^2)$, $\hat{V}_{\rm nc} = V_{\rm nc}/V_{*e}$, $V_{\rm nc} = V_{\theta i}^{\rm nc} - (\epsilon/q)V_{\varphi i}^{\rm nc}$, and $\xi = (L_s/\Gamma L_n)(\epsilon/q)$. Here, w is one-quarter of the full radial island width and

$$\rho = \frac{\rho_s}{w}, \tag{16}$$

$$\alpha = (1+\tau)^{1/2}\frac{w}{\rho_s}\frac{\Gamma L_n}{L_s}, \tag{17}$$

$$\delta_e = \frac{\beta_e(1+\tau)}{\alpha^2}, \tag{18}$$

where $\rho_s = (\Gamma T_e/m_i)^{1/2}/(eB_0/m_i)$ is the *ion sound gyroradius*, and $\beta_e = \Gamma\mu_0 n_0 T_e/B_0^2 \sim \epsilon^2 \ll 1$ is the *electron beta*. The *gyroradius parameter* ρ measures the ratio of the ion sound gyroradius to the island width. The *sound wave parameter* α gives the ratio of the parallel sound speed at the edge of the island to the diamagnetic velocity (which is the typical ion flow speed in the island frame). The island is said to be *subsonic* if $\alpha \gg 1$, *sonic* if $\alpha \sim 1$, and *supersonic* if $L_n/L_s \ll \alpha \ll 1$.[10] Since $\alpha \propto w$, it is clear that relatively narrow islands favor the supersonic regime, whereas relatively wide islands favor the subsonic regime. The *constant-ψ* parameter δ_e determines whether the ion polarization current flowing in the vicinity of the island is sufficiently strong to invalidate the constant-ψ approximation, with the approximation remaining valid provided $\delta_e \ll 1$ (assuming that the approximation has not already been invalidated by the solution in the outer region, i.e., assuming that $|\Delta' w| \ll 1$). In writing the above equations, it is assumed that $k_\theta w \ll 1$ (i.e., that the island is radially localized within the plasma), that $J_0 = B_0/(\mu_0 L_s)$, and that $\delta n/n_0 \to -x/L_n$ as $|x|/w \to \infty$. Here, L_s is termed the local equilibrium (i.e., unperturbed by the island) *magnetic shear length* and L_n is the local equilibrium *density gradient scale length*. Note that $L_s > 0$, $L_n > 0$, $q > 0$, $L_n/L_s \sim \epsilon/q \ll 1$, and $\xi \sim 1$ in a conventional large aspect-ratio low-β circular cross-section tokamak plasma equilibrium.

The four-field system of reduced neoclassical-MHD equations (10)–(13) is similar to that previously obtained by Furuya *et al.*[23] Within this system, ψ is the helical magnetic flux function, ϕ is the guiding center streamfunction (in a frame of reference corotating with the island), n is the perturbed electron number density, J is the perturbed parallel current density, and V is the parallel ion fluid velocity. Equation (10) is the parallel Ohm's law, Eq. (11) is the electron continuity equation (with contributions from the small, but non-negligible, divergence of the electron flow[22]), Eq. (12) is the parallel ion vorticity equation, and Eq. (13) is the parallel ion equation of motion.

In the limit $|x|/w \to 0$,

$$n \to X, \tag{19}$$

$$\phi \to vX, \tag{20}$$

$$V \to V_\infty, \tag{21}$$

where $v = \hat{V}_p - \hat{V}_{EB}$, $\hat{V}_{EB} = V_{EB}/V_{*e}$, $V_{EB} = B_0^{-1}(d\Phi/dx)_{|x|/w\to\infty}$, and V_∞ is a constant. Here, V_p and V_{EB} are the island phase velocity and the local equilibrium $\mathbf{E}\times\mathbf{B}$ velocity, respectively. Any radial shear in the equilibrium $\mathbf{E}\times\mathbf{B}$ velocity or the parallel ion velocity at the rational surface has been neglected. The *phase velocity parameter* v takes the values 1, 0, and $-\tau$ when the island propagates with the local equilibrium electron, guiding center, and ion fluids, respectively. (In unnormalized form: $V_p = V_{EB} + V_{*e}$, V_{EB}, and $V_{EB} - \tau V_{*e}$, respectively.) Of course, we expect $V_\infty = 0$ in a system in which toroidal flow damping plays a significant role (i.e., we expect the toroidal ion velocity to relax to its neoclassical value a long way from the island). Note that if toroidal flow damping is negligible, but poloidal flow damping non-negligible, then the large-$|X|$ boundary condition $V \to V_\infty$ (as opposed to $V \to V_\infty|X|$) is only valid when there is zero net electromagnetic force acting on the island region. Finally, the functions ϕ and n are clearly odd in X, while ψ, J, and V are clearly even.

F. Ordering

Equations (10)–(13) have been normalized in such a manner that

$$\psi, n, \phi, V, \hat{V}_p, \hat{V}_{\rm nc}, V_\infty, v \sim 1, \tag{22}$$

assuming that the ion fluid velocity (in the island rest frame) close to the island is the same order of magnitude as the electron diamagnetic velocity. In addition, we shall adopt the following ordering for the remaining nontransport parameters appearing in these equations:

$$1, \alpha, \tau, \xi \gg |\Delta' w|, \quad \delta_e, \quad \rho. \tag{23}$$

This ordering is consistent with a constant-ψ magnetic island lying in the so-called subsonic, sonic, or supersonic regimes (as opposed to the hypersonic regime) identified in Ref. 10. The ordering $\alpha, \tau \sim 1$ implies that $w \sim \epsilon^{-1}\rho_i \gg \rho_i$, where ρ_i is the ion Larmor radius. The plasma is assumed to be sufficiently collisional that trapped ions (whose orbit widths are also on the order of $\epsilon^{-1}\rho_i$) do not play a significant role in the island dynamics.[24] Hence, a fluid treatment of the ions is justified. The transport parameters $\hat{\eta}$, D, and $\hat{\mu}$ are assumed to be *very much smaller* than any other parameters in the problem, i.e.,

$$1 \ggg \hat{\eta}, \quad D, \quad \hat{\mu}, \tag{24}$$

which implies that the island is very much wider than a linear layer width. It is further assumed that $\hat{\nu}_\phi \sim (\epsilon/q)^2 \hat{\nu}_\theta \ll \hat{\nu}_\theta$. In other words, the toroidal flow damping rate is taken to be much smaller than the poloidal flow damping rate. This is reasonable since any toroidal variation in the magnetic field strength around flux surfaces which is induced by nonaxisymmetric error fields is likely to be much smaller in magnitude than the naturally occurring poloidal variation. Finally, it remains to order the poloidal flow damping rate $\hat{\nu}_\theta$ with respect to the transport parameters. We can identify three main ordering regimes. First, the *weak damping regime*,

$$1 \ggg \hat{\eta}, D, \hat{\mu}, \hat{\nu}_\theta \gg \hat{\nu}_\phi. \tag{25}$$

Second, the *intermediate damping regime*,

$$1 \ggg \hat{\nu}_\theta \gg \hat{\eta}, D, \hat{\mu}, \hat{\nu}_\phi. \tag{26}$$

Finally, the *strong damping regime*,

$$1, \hat{\nu}_\theta \gg \hat{\nu}_\phi \ggg \hat{\eta}, D, \hat{\mu}. \tag{27}$$

In this paper, we shall only investigate the first two damping regimes. Note that if the poloidal flow damping is due to classical parallel ion viscosity,[25] then $\hat{\nu}_\theta \sim \epsilon^2 l_i/\rho_i \sim \epsilon l_i/w$, where l_i is the ion mean free path. Thus, if the aspect ratio is sufficiently high and the plasma is sufficiently collisional, then it is possible for the system to lie in either the weak or the intermediate damping regimes (i.e., it is possible to have $\hat{\nu}_\theta \ll 1$). On the other hand, if the aspect ratio is low and the plasma is highly collisionless, then the system will always lie in the strong damping regime (i.e., $\hat{\nu}_\theta \gtrsim 1$). Furthermore, assuming $\hat{\nu}_\theta \ll 1$, and given that $\hat{\nu}_\theta$, $\hat{\nu}_\phi \propto w^0$, whereas $\hat{\eta}$, D, $\hat{\mu} \propto w^{-2}$, it is clear that relatively narrow islands favor the weak damping regime, whereas relatively wide islands favor the intermediate damping regime.

G. Constant-ψ approximation

The orderings $|\Delta' w|, \delta_e \ll 1$ imply that the well-known constant-ψ approximation[5] is valid [see Eq. (31)] so that Eq. (14) yields

$$\psi(X, \zeta) = -X^2/2 + \cos\zeta. \tag{28}$$

The above magnetic flux function maps out a helical magnetic island, centered on $X=0$. The O-point lies at $X=0$, $\zeta=0$, and $\psi=+1$, whereas the X-point lies at $X=0$, $\zeta=\pi$, and $\psi=-1$. The region lying inside the magnetic separatrix (which is situated at $\psi=-1$) corresponds to $+1>\psi>-1$, whereas the region lying outside the separatrix corresponds to $-1 \geq \psi > -\infty$. Finally, the full island width in the X-direction is 4. (Hence, the unnormalized width is $4w$.)

H. Flux-surface average operator

The *flux-surface average operator* is defined as the annihilator of $[A, \psi]$ for any A. It is easily shown that

$$\langle f(s,\psi,\zeta)\rangle = \oint \frac{f(s,\psi,\zeta)}{[2(-\psi+\cos\zeta)]^{1/2}} \frac{d\zeta}{2\pi} \tag{29}$$

outside the magnetic separatrix and

$$\langle f(s,\psi,\zeta)\rangle = \int_{-\zeta_0}^{\zeta_0} \frac{f(s,\psi,\zeta)+f(-s,\psi,\zeta)}{2[2(-\psi+\cos\zeta)]^{1/2}} \frac{d\zeta}{2\pi} \tag{30}$$

inside the separatrix, where $s=\mathrm{sgn}(X)$ and $\zeta_0=\cos^{-1}(\psi)$.

I. Rutherford equation

Standard asymptotic matching between the solutions in the inner and outer regions yields the *Rutherford island width evolution equation*,[6]

$$\frac{dw}{dt} \propto \mathrm{Re}(\Delta' w) + \delta_e J_c, \tag{31}$$

where Δ' is the linear tearing stability index,[5] and

$$J_c = 4\int_1^{-\infty} \langle J\cos\zeta\rangle d\psi. \tag{32}$$

The first term on the right-hand side of Eq. (31) parametrizes the contribution to the free energy available to drive the growth of the magnetic island which originates either from the outer region or the region external to the plasma, whereas

the second term parametrizes the corresponding contribution which originates from the inner region. The latter is usually ascribed to the *ion polarization current*.[26] Thus, the polarization current has a destabilizing effect on the island when the $\mathcal{O}(1)$ *ion polarization parameter* J_c is positive and vice versa.

J. Force balance

The parallel ion vorticity equation (12) can be written as

$$0 = \partial_X[\phi,\partial_X\phi] - \frac{\tau}{2}\{\partial_X^2[\phi,n] + \partial_X([\partial_X\phi,n] - [\phi,\partial_X n])\} - \frac{\partial J}{\partial X}\sin\zeta + \frac{\partial J}{\partial \zeta}X + \hat{\nu}_\theta\partial_X\{\xi V - \partial_X(\phi+\tau n)\} - \hat{\nu}_\varphi\xi\partial_X V + \hat{\mu}\partial_X^4(\phi+\tau n). \tag{33}$$

Operating on this expression with $\int_{-\infty}^{\infty}\oint(\cdots)Xd\zeta dX$, integrating by parts, and using the boundary conditions (19)–(21), we obtain

$$J_s = 4\int_1^{-\infty}\langle\hat{\nu}_\theta\{\xi(V-V_\infty) - \partial_X(\phi+\tau n) + v + \tau\} - \hat{\nu}_\varphi\xi(V-V_\infty)\rangle d\psi, \tag{34}$$

where

$$J_s = 4\int_1^{-\infty}\langle J\sin\zeta\rangle d\psi. \tag{35}$$

Furthermore, it is easily demonstrated from standard asymptotic matching that

$$\mathrm{Im}(\Delta' w) = \delta_e J_s. \tag{36}$$

Here, the left-hand side of the above equation represents the *net electromagnetic force* acting on the island region. This force acts in the *ion diamagnetic direction* $-\mathbf{k}$ when $\mathrm{Im}(\Delta' w)>0$ and in the *electron diamagnetic direction* $+\mathbf{k}$ when $\mathrm{Im}(\Delta' w)<0$. The right-hand side of (36) represents the component of the *net flow damping force* acting on the island region in the **k**-direction. Clearly, the electromagnetic and damping forces must balance in a steady state. Note that the boundary conditions (19)–(21) ensure that there is zero net Reynolds stress force or net ion viscous force acting on the island region in the **k**-direction. Now, for an *isolated* island—i.e., one which is not interacting electromagnetically with a resistive wall or a resonant error field—the net electromagnetic force acting on the island region is *zero*, i.e., $J_s=0$.[27] Hence, such an island satisfies

$$\int_1^{-\infty}\langle\hat{\nu}_\theta\{\xi(V-V_\infty) - \partial_X(\phi+\tau n) + v + \tau\} - \hat{\nu}_\varphi\xi(V-V_\infty)\rangle d\psi = 0. \tag{37}$$

This constraint implies that the component of the net flow damping force acting on the island region in the **k**-direction must be zero for an isolated island.

III. PRELIMINARY ANALYSIS

A. Introduction

In this section, we shall perform some preliminary analysis, which is common to both the weak and the intermediate damping regimes. In the following, our primary expansion is in the ratio of the normalized transport and damping terms to unity.

B. Zeroth-order equations

To lowest order in our primary expansion, we can neglect the transport and damping terms in Eqs. (10)–(13) to give

$$0 = [\phi^{(0)} - n^{(0)},\psi], \tag{38}$$

$$0 = [\phi^{(0)},n^{(0)}] + [V^{(0)} + \rho^2 J^{(0)},\psi], \tag{39}$$

$$0 = [\phi^{(0)},\partial_X^2\phi^{(0)}] - \frac{\tau}{2}\{\partial_X^2[\phi^{(0)},n^{(0)}] + [\partial_X^2\phi^{(0)},n^{(0)}] + [\partial_X^2 n^{(0)},\phi^{(0)}]\} + [J^{(0)},\psi], \tag{40}$$

$$0 = [\phi^{(0)},V^{(0)}] + \alpha^2[n^{(0)},\psi]. \tag{41}$$

Here, $\phi^{(0)}$ denotes the zeroth-order (in the primary expansion) component of ϕ, etc. All of the quantities appearing in the above equations are of the order of unity except for ρ^2, which is much less than unity [see Eq. (23)]. Adopting the following secondary expansions:

$$\phi^{(0)} = s[\phi_0(\psi) + \rho^2\phi_1], \tag{42}$$

$$n^{(0)} = s[n_0(\psi) + \rho^2 n_1], \tag{43}$$

$$V^{(0)} = V_0(\psi) + \rho^2 V_1, \tag{44}$$

with $\phi_0,\phi_1,n_0,n_1,V_0,V_1\sim 1$ and $\langle\phi_1\rangle=\langle n_1\rangle=\langle V_1\rangle=0$, we find that

$$\phi_1 = n_1 = -\frac{[M(M+\tau L)/2]'\widetilde{X^2}}{L - M + (\alpha^2 + V_0')/M}, \tag{45}$$

$$V_1 = \left(\frac{\alpha^2 + V_0'}{M}\right)\phi_1, \tag{46}$$

$$J^{(0)} = [M(M+\tau L)/2]'\widetilde{X^2} + J_0(\psi), \tag{47}$$

where $M\equiv d\phi_0/d\psi$, $L\equiv dn_0/d\psi$, $'\equiv d/d\psi$, and $\tilde{A}\equiv A-\langle A\rangle/\langle 1\rangle$. However, the flux-surface average of Eq. (10) gives $\langle J\rangle=0$. Hence, we conclude that $J_0=0$ and

$$J^{(0)} = [M(M+\tau L)/2]'\widetilde{X^2}. \tag{48}$$

The above equation specifies how an *ion polarization current* is generated by sheared ion flow in the vicinity of the island (in the island rest frame). It remains to determine the three

profile functions: $M(\psi)$, $L(\psi)$, and $V_0(\psi)$. This can only be achieved by incorporating the transport and damping terms into our analysis.[28,29]

C. First-order equations

To first order in our primary expansion, Eqs. (10)–(13) give

$$0=[\phi^{(1)}-n^{(1)},\psi]+\delta_e\hat{\eta}J^{(0)}, \tag{49}$$

$$0=[\phi^{(1)},n^{(0)}]+[\phi^{(0)},n^{(1)}]+[V^{(1)}+\rho^2J^{(1)},\psi]+D\partial_X^2n^{(0)}, \tag{50}$$

$$\begin{aligned}0=&[\phi^{(1)},\partial_X^2\phi^{(0)}]+[\phi^{(0)},\partial_X^2\phi^{(1)}]-\frac{\tau}{2}\\&\times\{\partial_X^2[\phi^{(1)},n^{(0)}]+\partial_X^2[\phi^{(0)},n^{(1)}]+[\partial_X^2\phi^{(1)},n^{(0)}]\\&+[\partial_X^2\phi^{(0)},n^{(1)}]+[\partial_X^2n^{(1)},\phi^{(0)}]+[\partial_X^2n^{(0)},\phi^{(1)}]\}\\&+[J^{(1)},\psi]+\hat{\nu}_\theta\partial_X\{\xi V^{(0)}-\partial_X(\phi^{(0)}+\tau n^{(0)})\}-\hat{\nu}_\phi\xi\partial_XV^{(0)}\\&+\hat{\mu}\partial_X^4(\phi^{(0)}+\tau n^{(0)}),\end{aligned} \tag{51}$$

$$\begin{aligned}0=&[\phi^{(1)},V^{(0)}]+[\phi^{(0)},V^{(1)}]+\alpha^2[n^{(1)},\psi]\\&-\hat{\nu}_\theta(\epsilon/q)^2\xi^{-1}\{\xi V^{(0)}-\partial_X(\phi^{(0)}+\tau n^{(0)})+v+\hat{V}_{EB}-\hat{V}_{\rm nc}\}\\&-\hat{\nu}_\phi V^{(0)}+\hat{\mu}\partial_X^2V^{(0)}.\end{aligned} \tag{52}$$

To lowest order in our secondary expansion, these equations reduce to

$$0=[\phi^{(1)}-n^{(1)},\psi], \tag{53}$$

$$0=[\phi^{(1)},n_0]+[\phi_0,n^{(1)}]+[V^{(1)},\psi]+D\partial_X^2n_0, \tag{54}$$

$$\begin{aligned}0=&[\phi^{(1)},\partial_X^2\phi_0]+[\phi_0,\partial_X^2\phi^{(1)}]-\frac{\tau}{2}\\&\times\{\partial_X^2[\phi^{(1)},n_0]+\partial_X^2[\phi_0,n^{(1)}]\ \ +[\partial_X^2\phi^{(1)},n_0]\\&+[\partial_X^2\phi_0,n^{(1)}]+[\partial_X^2n^{(1)},\phi_0]+[\partial_X^2n_0,\phi^{(1)}]\}+[J^{(1)},\psi]\\&+\hat{\nu}_\theta\partial_X\{\xi V_0-\partial_X(\phi_0+\tau n_0)\}-\hat{\nu}_\phi\xi\partial_XV_0+\hat{\mu}\partial_X^4\\&\times(\phi_0+\tau n_0),\end{aligned} \tag{55}$$

$$\begin{aligned}0=&[\phi^{(1)},V_0]+[\phi_0,V^{(1)}]+\alpha^2[n^{(1)},\psi]-\hat{\nu}_\theta(\epsilon/q)^2\xi^{-1}\\&\times\{\xi V_0-\partial_X(\phi_0+\tau n_0)+v+\hat{V}_{EB}-\hat{V}_{\rm nc}\}-\hat{\nu}_\phi V_0\\&+\hat{\mu}\partial_X^2V_0.\end{aligned} \tag{56}$$

D. Inside separatrix

Inside the separatrix, we must have $\phi_0(\psi)=n_0(\psi)=0$ since it is impossible for a nonzero flux-surface function to be odd in X. It follows that $L(\psi)=M(\psi)=0$. Furthermore, Eqs. (53)–(56) give

$$V_0=-\left[\frac{\hat{\nu}_\theta(\epsilon/q)^2}{\hat{\nu}_\theta(\epsilon/q)^2+\hat{\nu}_\phi}\right]\xi^{-1}(v+\hat{V}_{EB}-\hat{V}_{\rm nc}), \tag{57}$$

with $\phi^{(1)}=n^{(1)}=V^{(1)}=J^{(1)}=0$.

E. Outside separatrix

Outside the separatrix, Eqs. (53), (55), and (56) yield

$$[\phi^{(1)},\psi]=[n^{(1)},\psi]=\frac{-(DML'+\hat{\mu}V_0'')\widetilde{X^2}+\hat{\nu}_\theta(\epsilon/q)^2\xi^{-1}(M+\tau L)\widetilde{X}}{M(L-M)+\alpha^2+V_0'} \tag{58}$$

and

$$[V^{(1)},\psi]=\frac{[-D(\alpha^2+V_0')L'+\hat{\mu}(L-M)V_0'']\widetilde{X^2}-\hat{\nu}_\theta(\epsilon/q)^2\xi^{-1}(L-M)(M+\tau L)\widetilde{X}}{M(L-M)+\alpha^2+V_0'}. \tag{59}$$

Moreover, the flux-surface average of Eq. (54) reduces to

$$\frac{d}{d\psi}(\langle X^2\rangle L)=0. \tag{60}$$

This equation can be solved, subject to the boundary condition (19), to give

$$L(\psi)=-\frac{1}{\langle X^2\rangle}. \tag{61}$$

It follows that the profile function $L(\psi)$ is *discontinuous* across the separatrix. In fact, $L=0$ just inside the separatrix, whereas $L=-\pi/4$ just outside the separatrix. The discontinuity in $L(\psi)$ drives a similar discontinuity in the profile function $M(\psi)$ (see Appendix B). The flux-surface average of Eq. (56) yields

$$\frac{d}{d\psi}\left(\langle X^2\rangle\frac{dV_0}{d\psi}\right)-\frac{\hat{\nu}_\theta}{\hat{\mu}}\left(\frac{\epsilon}{q}\right)^2\xi^{-1}[(\xi V_0+v+\hat{V}_{EB}-\hat{V}_{\rm nc})\langle 1\rangle+M+\tau L]-\frac{\hat{\nu}_\phi}{\hat{\mu}}V_0\langle 1\rangle=0. \tag{62}$$

Finally, the flux-surface average of Eq. (55) gives

$$0 = \langle[\phi^{(1)}, M'\widetilde{X^2}]\rangle + \frac{\tau}{2}\{\langle[\phi^{(1)}, M'\widetilde{X^2}]\rangle + \langle[\phi^{(1)}, L'\widetilde{X^2}]\rangle\}$$
$$- \frac{\tau}{2}\frac{d}{d\psi}\{\langle X^2(\{L-M\}[\phi^{(1)},\psi])_\psi\rangle\} - \hat{\nu}_\theta \frac{d}{d\psi}$$
$$\times\{\xi V_0 + (M+\tau L)\langle X^2\rangle\} + \hat{\nu}_\phi \frac{d}{d\psi}(\xi V_0)$$
$$+ \hat{\mu}\frac{d^2}{d\psi^2}\left\{\langle X^4\rangle \frac{d}{d\psi}(M+\tau L)\right\}, \tag{63}$$

where the subscript ψ denotes $\partial/\partial\psi|_\zeta$. However,

$$\langle[\phi^{(1)}, M'\widetilde{X^2}]\rangle \equiv \frac{d}{d\psi}\langle M'\widetilde{X^2}[\phi^{(1)},\psi]\rangle, \tag{64}$$

$$\langle X^2[M\phi^{(1)},\psi]_\psi\rangle \equiv \frac{d}{d\psi}\langle\widetilde{X^2}[M\phi^{(1)},\psi]\rangle. \tag{65}$$

Hence, using Eq. (58), we obtain

$$0 = \frac{d}{d\psi}\left\{-[M' + (\tau/2)(L'+M')]H + \frac{d}{d\psi}\right.$$
$$\times[(\tau/2)(L-M)H] - \frac{\hat{\nu}_\theta}{\hat{\mu}}[\xi V_0 + (M+\tau L)\langle X^2\rangle]$$
$$\left. + \frac{\hat{\nu}_\phi}{\hat{\mu}}\xi V_0 + \frac{d}{d\psi}\left[\langle X^4\rangle\frac{d}{d\psi}(M+\tau L)\right]\right\}, \tag{66}$$

where

$$H(\psi) = \frac{[(D/\hat{\mu})ML' + V_0'']\langle\widetilde{X^2}\widetilde{X^2}\rangle - (\hat{\nu}_\theta/\hat{\mu})(\epsilon/q)^2\xi^{-1}(M+\tau L)\langle\widetilde{X^2}\widetilde{X}\rangle}{M(L-M) + \alpha^2 + V_0'}. \tag{67}$$

Equation (66) can be integrated, subject to the boundary conditions (19)–(21), to give

$$0 = \frac{d}{d\psi}\left[\langle X^4\rangle\frac{d}{d\psi}(M+\tau L) + (\tau/2)(L-M)H\right]$$
$$-[M' + (\tau/2)(L'+M')]H - \frac{\hat{\nu}_\theta}{\hat{\mu}}$$
$$\times[\xi(V_0 - V_\infty) + v + \tau + (M+\tau L)\langle X^2\rangle]$$
$$+ \frac{\hat{\nu}_\phi}{\hat{\mu}}\xi(V_0 - V_\infty). \tag{68}$$

Equations (61), (62), and (68) determine the three profile functions $L(\psi)$, $V_0(\psi)$, and $M(\psi)$, respectively, in the region outside the separatrix.

Now, it is easily demonstrated that

$$\frac{V_{\theta i} - V_{\theta i}^{\rm nc}}{V_{*e}} = X(M+\tau L) + \xi(V_0 - V_\infty), \tag{69}$$

$$\frac{V_{\varphi i} - V_{\varphi i}^{\rm nc}}{V_{*e}} = \frac{q}{\varepsilon}\xi V_0, \tag{70}$$

where $V_{\theta i} = \mathbf{V}_i\cdot\mathbf{e}_\theta$, etc. Thus, the profile functions $M(\psi)$, $L(\psi)$, and $V_0(\psi)$ effectively specify the ion poloidal and toroidal velocity profiles in the vicinity of the island. Moreover,

$$\frac{V_{ki} - V_p}{V_{*e}} = X(M+\tau L), \tag{71}$$

where $V_{ki} = \mathbf{V}_i\cdot\mathbf{k}$. As is clear from the above equation, the fact that $M=L=0$ inside the separatrix implies that the ion fluid within the separatrix propagates at the same velocity as the island in the $\mathbf{k}$-direction.

IV. WEAK DAMPING REGIME

A. Analysis

The weak damping regime is governed by the ordering scheme (25). Within this scheme, it is consistent to completely neglect toroidal flow damping and to also neglect $\hat{\nu}_\theta(\epsilon/q)^2$ with respect to $\hat{\mu}$ outside the island separatrix.

It follows from Eq. (57) that

$$V_0 = -\xi^{-1}(v + \hat{V}_{EB} - \hat{V}_{\rm nc}) \tag{72}$$

inside the separatrix. Outside the separatrix, Eq. (62) reduces to

$$\frac{d}{d\psi}\left(\langle X^2\rangle\frac{dV_0}{d\psi}\right) = 0. \tag{73}$$

The solution, subject to the boundary condition (21), is

$$V_0 = V_\infty, \tag{74}$$

where V_∞ is an arbitrary constant. (Here, we are implicitly assuming that the island is isolated.) Now, $V_0(\psi)$ must be continuous across the separatrix, otherwise the V_0'' term in Eq. (67) would become too large to be balanced by any other terms in Eq. (68). Moreover, it is clear from Eq. (62) that the discontinuities in the profile functions $L(\psi)$ and $M(\psi)$ across the island separatrix do not drive strong gradients in $V_0(\psi)$. Hence, the above equations yield

$$\hat{V}_{EB} = \hat{V}_{\rm nc} - v - \xi V_\infty. \tag{75}$$

It follows that the (normalized) local equilibrium $\mathbf{E}\times\mathbf{B}$ velocity $\hat{V}_{EB}$ is undetermined to an arbitrary constant (i.e., V_∞). This merely reflects the fact that the local equilibrium toroidal ion fluid velocity is *unconstrained* in the absence of toroidal flow damping.

Equation (68) reduces to

$$0 = \frac{d}{d\psi}\left[\langle X^4\rangle \frac{d}{d\psi}(M+\tau L) + (\tau/2)(L-M)H\right] - [M' + (\tau/2)(L'+M')]H - \frac{\hat{\nu}_\theta}{\hat{\mu}} \times [(M+\tau L)\langle X^2\rangle + v + \tau], \tag{76}$$

where $' \equiv d/d\psi$ and

$$H(\psi) = \frac{D}{\hat{\mu}} \frac{ML'}{M(L-M)+\alpha^2}\langle \widetilde{X^2}\widetilde{X^2}\rangle. \tag{77}$$

The boundary condition on $M(\psi)$ just outside the separatrix is obtained by integrating Eq. (76) across the separatrix using the fact that $M=L=0$ just inside the separatrix, whereas $L=-\pi/4$ just outside the separatrix (see Appendix B). The boundary condition a long way from the separatrix is [see Eq. (20)]

$$M(\psi \to -\infty) = -\frac{v}{\sqrt{-2\psi}}. \tag{78}$$

The imposition of this boundary condition implies the elimination of an exponentially growing solution which varies as $\exp[\sqrt{(\hat{\nu}_\theta/\hat{\mu})(-2\psi)}]$. The solution of Eq. (76), subject to the abovementioned boundary conditions, uniquely determines the profile function $M(\psi)$ in the region beyond the separatrix.

For an isolated island, the island phase velocity parameter v is set by the force balance constraint (37), which reduces to

$$(v+\tau)\int_1^{-1}\langle 1\rangle d\psi + \int_{-1}^{-\infty}[M+\tau L+(v+\tau)\langle 1\rangle]d\psi = 0. \tag{79}$$

Thus, the (normalized) island phase velocity in the laboratory frame is

$$\hat{V}_p = \hat{V}_{EB} + v = \hat{V}_{\rm nc} - \xi V_\infty. \tag{80}$$

Note that $\hat{V}_p$ is arbitrary (since V_∞ is also arbitrary). This simply reflects the fact that the island phase velocity can take any value in a plasma which is free to rotate toroidally. In particular, if the island is *locked* to a resonant error field so that $\hat{V}_p=0$, then this additional constraint can be incorporated into the above analysis by setting $V_\infty=\xi^{-1}\hat{V}_{\rm nc}$. No further changes are necessary. In other words, if the island is locked, then the local equilibrium toroidal ion fluid velocity is free to adjust itself to allow for this fact without the need to introduce any additional flows in the vicinity of the island [i.e., without the need to change the profile function $M(\psi)$]. It should be noted that any change in the local equilibrium toroidal ion fluid velocity required to lock the island is resisted by plasma perpendicular viscosity in the outer region, and that this resistance must be overcome by the electromagnetic force due to the error field before locking can occur.[27] The required change in toroidal velocity also generally gives rise to sheared flow in the outer region which can drive a very small polarization current in the vicinity of the island. This effect, which is neglected in this paper, is discussed in Ref. 30.

Finally, the ion polarization parameter J_c [see Eq. (31)] is given by [see Eqs. (32) and (48)]

$$J_c = 2\int_{-1}^{-\infty}[M(M+\tau L)/2]'\langle \widetilde{X^2}\widetilde{X^2}\rangle d\psi. \tag{81}$$

It follows, from the above discussion, that the polarization term in the Rutherford equation of a locked island which lies in the weak damping regime is the same as that for a comparable isolated island (subject to the caveat mentioned above).

B. Numerical results

1. Introduction

Equation (76) can be solved numerically, subject to the said boundary conditions, to give the profile function $M(\psi)$ in the region beyond the island separatrix. Once this has been achieved, the island phase velocity parameter v can be determined from the constraint (79) and the ion polarization parameter J_c can be calculated from Eq. (81). The details of the procedure used to determine $M(\psi)$, v, and J_c are given in Appendix B.

2. Negligible damping regime

Before discussing the effect of weak flow damping on an isolated island, it is worthwhile to review the case in which flow damping is either absent or completely negligible.[10] In the absence of flow damping (i.e., $\hat{\nu}_\theta=0$), the procedure outlined in Appendix B must be slightly modified because the asymptotic behavior of $M(\psi)$ a long way from the separatrix is changed (i.e., there are no longer any exponential solutions). In fact, the most general solution for M in the limit $\psi\to-\infty$ becomes

$$M(\psi \to -\infty) = \frac{M_0}{\sqrt{-2\psi}} + M_1, \tag{82}$$

where M_0 and M_1 are arbitrary constants. In the limit $\hat{\nu}_\theta\to 0$, the constraint integral (79) must remain finite, otherwise the net flow damping force acting on the island region would not tend to zero, as should be the case. However, it is easily seen that the integral (79) only remains finite provided that

$$M_1 = 0, \tag{83}$$

$$M_0 = -v. \tag{84}$$

Thus, the modified procedure for calculating the phase velocity parameter v is to solve Eq. (76) subject to the boundary condition (83) instead of Eq. (78). This uniquely determines the parameter M_0. The phase velocity parameter is then given by the relation $v=-M_0$. Of course, our modified procedure is exactly the same as that used in Ref. 10 to determine the phase velocity of an isolated magnetic island in the absence of flow damping. In fact, the modified criterion is equivalent to saying that there is *zero net ion viscous force* acting on the island region in the **k**-direction (since it is

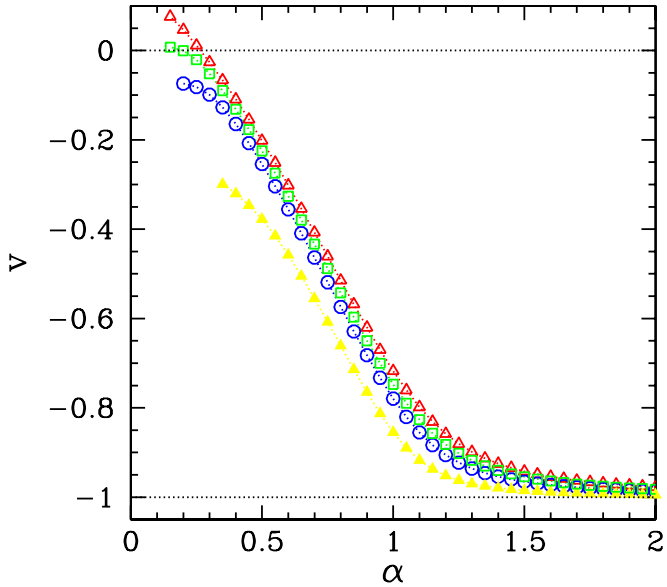

FIG. 1. (Color online) The island phase velocity parameter v calculated as a function of the sound wave parameter α for an isolated island in the absence of flow damping with various values of the separatrix layer width parameter, δ_s. The red (open triangle), green (open square), blue (open circle), and yellow (solid triangle) curves correspond to $\delta_s=0$, 10^{-9}, 10^{-6}, and 10^{-3}, respectively. The values of the other parameters used in the calculations are $\tau=1$ and $D/\hat{\mu}=1$.

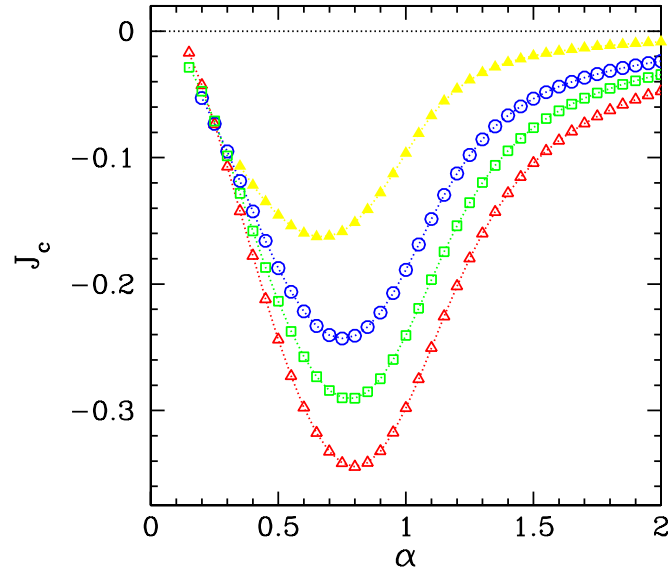

FIG. 2. (Color online) The ion polarization parameter J_c calculated as a function of the sound wave parameter α for an isolated island in the absence of flow damping with various values of the separatrix layer width parameter, δ_s. The red (open triangle), green (open square), blue (open circle), and yellow (solid triangle) curves correspond to $\delta_s=0$, 10^{-9}, 10^{-6}, and 10^{-3}, respectively. The values of the other parameters used in the calculations are $\tau=1$ and $D/\hat{\mu}=1$.

easily shown that the net viscous force is proportional to M_1). In conclusion, our new procedure for determining the island phase velocity in the presence of flow damping is fully consistent with our old procedure for determining this velocity in the absence of damping.

The red curves in Figs. 1 and 2 illustrate the standard case discussed in Ref. 10. According to Fig. 1, an isolated undamped island propagates with the local equilibrium ion fluid (i.e., $v\simeq-\tau$) in the subsonic regime ($\alpha\gg1$), with the local equilibrium guiding center fluid (i.e., $v\simeq0$) in the supersonic regime ($\alpha\ll1$), and at some intermediate velocity in the sonic regime ($\alpha\sim1$). Moreover, according to Fig. 2, the ion polarization current has a *stabilizing* effect on the island (i.e., $J_c<0$). This effect peaks in the sonic regime and is relatively small in the subsonic and supersonic regimes.

Now, the terms appearing in Eq. (76), which involve the function $H(\psi)$ clearly, describe a *resonance* between the ion flow in the vicinity of the island and the sound wave. In fact, if these terms are omitted then Eq. (76) possesses a fairly obvious solution, i.e., $M=-\tau L$, and $v=-\tau$. This solution corresponds to an island that propagates with the local equilibrium ion fluid and has no ion flow in the island rest frame. The lack of ion flow in the rest frame immediately implies that there is no ion polarization current and hence that $J_c=0$. In other words, in the absence of the sound wave resonance, we expect $v=-\tau$ and $J_c=0$. Thus, any deviation from this result can be ascribed to the influence of the sound wave resonance.

As mentioned previously, the profile functions $L(\psi)$ and $M(\psi)$ are both discontinuous across the island separatrix. These discontinuities are resolved in a thin boundary layer of (normalized) thickness $\delta_s\sim\rho\ll1$ (see Appendix B). As is well known, the ion polarization current flowing in the boundary layer makes the dominant contribution to the ion polarization parameter J_c.[30] Now, the calculations discussed in Ref. 10 are all performed under the assumption that the separatrix layer is infinitely thin, i.e., that $\delta_s=0$. The nonred curves in Figs. 1 and 2 show the results of more realistic calculations in which the separatrix layer has a small but finite thickness, i.e., $0<\delta_s\ll1$. It can be seen that a finite separatrix layer thickness makes little difference to the island phase velocity parameter but leads to a significant reduction in the magnitude of the ion polarization parameter. In fact, the reduction scales approximately as $1/|\ln\delta_s|$. This effect is due to a suppression of the ion polarization current flowing in the separatrix layer which can ultimately be traced back to the rapid variation of the flux-surface function $\langle 1\rangle$ in the vicinity of the separatrix (see Appendix A). (In fact, $\langle 1\rangle$ has a logarithmic singularity at the separatrix.) We conclude that calculations which neglect the finite thickness of the separatrix layer tend to *overestimate* the stabilizing effect of the ion polarization current.

3. Weak damping regime

The effect of weak flow damping on an isolated magnetic island is illustrated in Figs. 3 and 4. Here, the parameters v and J_c are calculated according to the procedure set out in Appendix B. (Apart from the $\hat{\nu}_\theta=0$ case, for which the calculation is performed using the modified procedure discussed above.) Unfortunately, it becomes increasingly difficult, from a numerical point of view, to find low-α solutions as the so-called *weak damping parameter*, $\hat{\nu}_\theta/\hat{\mu}$, increases, which accounts for the lack of low-α/high-$\hat{\nu}_\theta/\hat{\mu}$ data points in the figures. According to Fig. 3, if $\hat{\nu}_\theta/\hat{\mu}$ is small compared

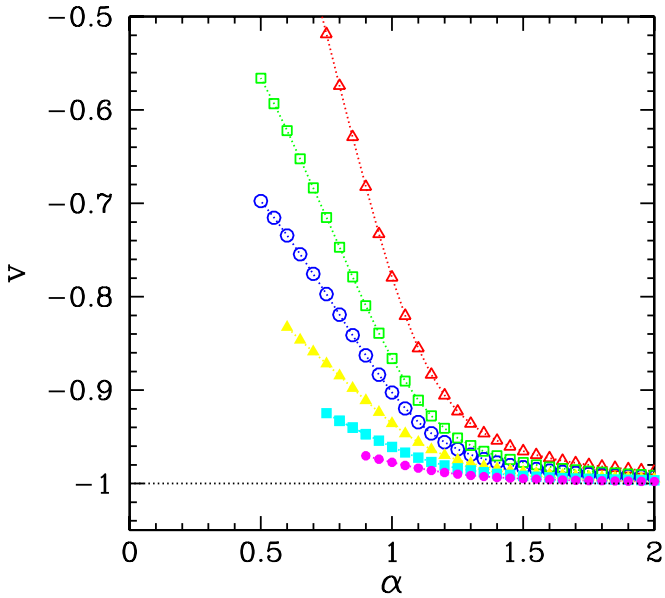

FIG. 3. (Color online) The island phase velocity parameter v calculated as a function of the sound wave parameter α for an isolated island in the weak damping regime with various values of the weak damping parameter, $\hat{\nu}_\theta/\hat{\mu}$. The red (open triangle), green (open square), blue (open circle), yellow (solid triangle), cyan (solid square), and magenta (solid circle) curves correspond to $\hat{\nu}_\theta/\hat{\mu}=0$, 0.25, 1, 4, 16, and 64, respectively. The values of the other parameters used in the calculations are $\tau=1$, $D/\hat{\mu}=1$, and $\delta_s=10^{-6}$.

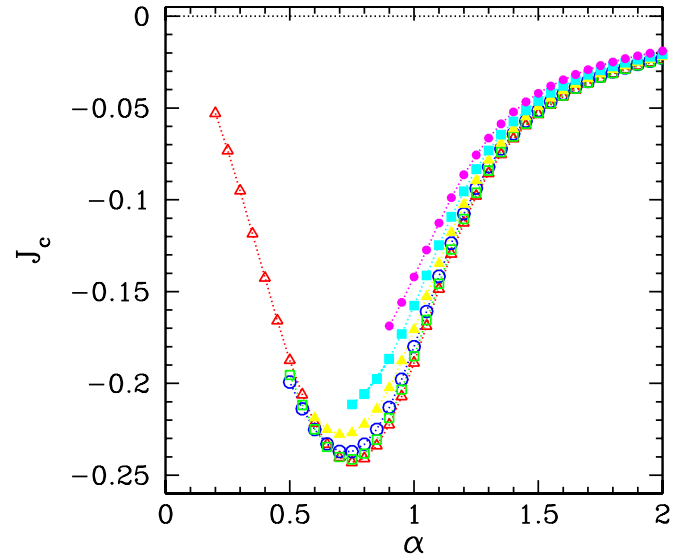

FIG. 4. (Color online) The ion polarization parameter J_c calculated as a function of the sound wave parameter α for an isolated island in the weak damping regime with various values of the weak damping parameter, $\hat{\nu}_\theta/\hat{\mu}$. The red (open triangle), green (open square), blue (open circle), yellow (solid triangle), cyan (solid square), and magenta (solid circle) curves correspond to $\hat{\nu}_\theta/\hat{\mu}=0$, 0.25, 1, 4, 16, and 64, respectively. The values of the other parameters used in the calculations are $\tau=1$, $D/\hat{\mu}=1$, and $\delta_s=10^{-6}$.

to unity, then the value of the island phase velocity parameter v remains close to that obtained in the absence of damping. However, as $\hat{\nu}_\theta/\hat{\mu}$ increases and becomes large compared to unity, v tends toward $-\tau$. In other words, sufficiently high levels of flow damping counteract the influence of the sound wave resonance and force the island to propagate with the local equilibrium ion fluid.[31] According to Fig. 4, flow damping has surprisingly little effect on the ion polarization parameter J_c. Indeed, there is only a modest reduction in J_c when $\hat{\nu}_\theta/\hat{\mu}\gg 1$. At first sight, this seems a somewhat paradoxical result since flow damping suppresses the sheared ion flow in the vicinity of the island (in the island rest frame) which is needed to generate an ion polarization current by relaxing the flow to its neoclassical value. However, the paradox can be resolved by recalling that the dominant contribution to J_c comes from a thin boundary layer of (normalized) thickness $\delta_s\sim\rho\ll 1$ located on the island separatrix. The explanation for the behavior shown in Fig. 4 is that the sheared ion flow in the region beyond the separatrix is increasingly suppressed as $\hat{\nu}_\theta/\hat{\mu}$ becomes large compared to unity, but the sheared flow within the separatrix layer is largely unaffected. Hence, as $\hat{\nu}_\theta/\hat{\mu}$ increases, the contribution of the separatrix layer to J_c persists, long after that from the region beyond the separatrix has been eliminated by flow damping.

4. Weak/intermediate damping regime

Now, in the limit in which the weak damping parameter, $\hat{\nu}_\theta/\hat{\mu}$, is very much larger than unity, we expect the poloidal ion flow in the region beyond the separatrix to relax to its neoclassical value everywhere apart from a thin region located just outside the separatrix with (normalized) thickness of $\sim\sqrt{\hat{\mu}/\hat{\nu}_\theta}$. Furthermore, when the width of this region becomes comparable to the width δ_s of the aforementioned separatrix boundary layer, we expect flow damping to start to suppress the sheared ion flow within the boundary layer and, hence, to eliminate the contribution of the layer to J_c. We shall refer to this regime, which is characterized by $\hat{\nu}_\theta/\hat{\mu}\sim\delta_s^{-2}\gg 1$, as the *weak/intermediate damping regime*. A suitable procedure for determining the island phase velocity parameter v and the ion polarization parameter J_c in the weak/intermediate regime is described in Appendix C.

The effect of weak/intermediate flow damping on an isolated magnetic island is illustrated in Figs. 5 and 6. It can be seen that as the so-called weak/intermediate damping parameter, $4\delta_s^2\hat{\nu}_\theta/\hat{\mu}$, approaches unity, the island phase velocity parameter is forced toward the value $-\tau$ even in the supersonic regime, and the ion polarization parameter is strongly reduced, particularly in the subsonic regime. There seems little doubt, from the figure, that in the limit that $4\delta_s^2\hat{\nu}_\theta/\hat{\mu}$ becomes much greater than unity (which, unfortunately, is difficult to deal with numerically), $v\to-\tau$ and $J_c\to 0$. Of course, these parameter values correspond to an island solution which propagates with the local equilibrium ion fluid and which experiences no stabilizing effect from the ion polarization current (since there is no sheared ion flow in the island rest frame).

V. INTERMEDIATE DAMPING REGIME

A. Analysis

The intermediate damping regime is governed by the ordering scheme (26). Note that toroidal flow damping is retained within this scheme. It follows that the constant V_∞, appearing in the boundary condition (21), must be set to zero

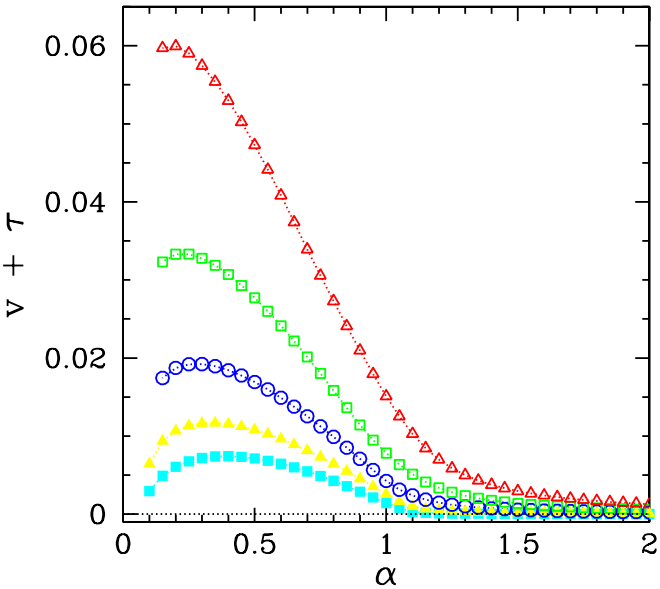

FIG. 5. (Color online) The island phase velocity parameter v calculated as a function of the sound wave parameter α for an isolated island in the weak/intermediate damping regime with various values of the weak/intermediate damping parameter, $4\delta_s^2\hat{\nu}_\theta/\hat{\mu}$. The red (open triangle), green (open square), blue (open circle), yellow (solid triangle), and cyan (solid square) curves correspond to $4\delta_s^2\hat{\nu}_\theta/\hat{\mu}=9.77\times10^{-4}$, 3.91×10^{-3}, 1.56×10^{-2}, 6.25×10^{-2}, and 0.25, respectively. The values of the other parameters used in the calculations are $\tau=1$, $D/\hat{\mu}=1$, and $\delta_s=10^{-3}$.

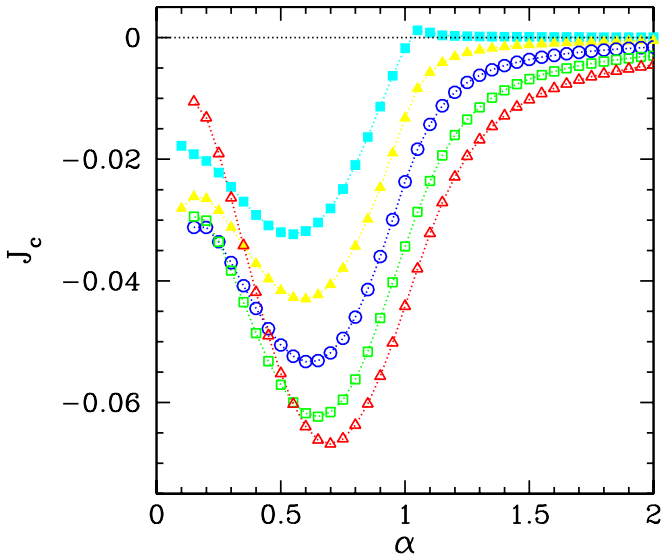

FIG. 6. (Color online) The ion polarization parameter J_c calculated as a function of the sound wave parameter α for an isolated island in the weak/intermediate damping regime with various values of the weak/intermediate damping parameter, $4\delta_s^2\hat{\nu}_\theta/\hat{\mu}$. The red (open triangle), green (open square), blue (open circle), yellow (solid triangle), and (solid square) cyan curves correspond to $4\delta_s^2\hat{\nu}_\theta/\hat{\mu}=9.77\times10^{-4}$, 3.91×10^{-3}, 1.56×10^{-2}, 6.25×10^{-2}, and 0.25, respectively. The values of the other parameters used in the calculations are $\tau=1$, $D/\hat{\mu}=1$, and $\delta_s=10^{-3}$.

so as to ensure that the toroidal ion velocity relaxes to its neoclassical value a long way from the island.

According to Eq. (57),

$$\xi V_0 = -\left[\frac{\hat{\nu}_\theta(\epsilon/q)^2}{\hat{\nu}_\theta(\epsilon/q)^2+\hat{\nu}_\phi}\right](v+\hat{V}_{EB}-\hat{V}_{\rm nc}) \tag{85}$$

inside the separatrix. Outside the separatrix, the dominant poloidal flow damping term in Eq. (68) yields

$$\xi V_0 = -F\langle X^2\rangle - (v+\tau), \tag{86}$$

where

$$F(\psi) = M(\psi) + \tau L(\psi). \tag{87}$$

The boundary conditions (19) and (20) imply that

$$F(\psi\to-\infty) = -\frac{(v+\tau)}{\sqrt{-2\psi}} \tag{88}$$

a long way from the separatrix.

Substituting Eq. (86) into Eq. (62), we obtain

$$0 = \frac{d}{d\psi}\left[\langle X^2\rangle\frac{d}{d\psi}(\langle X^2\rangle F)\right] - \frac{\hat{\nu}_\theta}{\hat{\mu}}\left(\frac{\epsilon}{q}\right)^2[F(\langle X^2\rangle\langle 1\rangle - 1) + (\tau+\hat{V}_{\rm nc}-\hat{V}_{EB})\langle 1\rangle] - \frac{\hat{\nu}_\phi}{\hat{\mu}}[F\langle X^2\rangle + v + \tau]\langle 1\rangle. \tag{89}$$

However, it is clear, from an examination of the above equation, that the boundary condition (88) can only be satisfied provided that

$$\hat{V}_{EB} = \hat{V}_{\rm nc} + \tau. \tag{90}$$

This restriction merely reflects the fact that the local equilibrium $\mathbf{E}\times\mathbf{B}$ velocity is constrained to take a fixed value, determined from neoclassical theory, in the presence of both poloidal and toroidal flow damping. Thus, Eq. (85) yields

$$\xi V_0 = -\left[\frac{\hat{\nu}_\theta(\epsilon/q)^2}{\hat{\nu}_\theta(\epsilon/q)^2+\hat{\nu}_\phi}\right](v+\tau) \tag{91}$$

inside the separatrix, whereas Eq. (89) reduces to

$$0 = \frac{d}{d\psi}\left[\langle X^2\rangle\frac{d}{d\psi}(\langle X^2\rangle F)\right] - \frac{\hat{\nu}_\theta}{\hat{\mu}}\left(\frac{\epsilon}{q}\right)^2 F[\langle X^2\rangle\langle 1\rangle - 1] - \frac{\hat{\nu}_\phi}{\hat{\mu}}[F\langle X^2\rangle + v + \tau]\langle 1\rangle \tag{92}$$

outside the separatrix. The boundary condition just outside the separatrix follows from Eqs. (86) and (91), and the requirement that $V_0(\psi)$ be continuous across the separatrix, i.e.,

$$F(\psi=-1) = -\frac{\pi}{4}\left[\frac{\hat{\nu}_\phi}{\hat{\nu}_\theta(\epsilon/q)^2+\hat{\nu}_\phi}\right](v+\tau). \tag{93}$$

Again, V_0 must be continuous across the separatrix because the V_0'' term in Eq. (67) would otherwise become too large to be balanced by any other terms in Eq. (68). The solution of Eq. (92), subject to the boundary conditions (88) and (93), uniquely determines the profile function $F(\psi)$ [and, hence, the profile function $M(\psi)$] in the region beyond the separatrix.

For an isolated island, the island phase velocity parameter v is set by the force balance constraint (37), which reduces to

$$\left[\frac{\hat{\nu}_\phi}{\hat{\nu}_\theta(\epsilon/q)^2+\hat{\nu}_\phi}\right](v+\tau)\int_1^{-1}\langle 1\rangle d\psi - \int_{-1}^{\infty} F[\langle X^2\rangle\langle 1\rangle - 1]d\psi = 0. \tag{94}$$

Finally, the ion polarization parameter J_c is given by [see Eq. (81)]

$$J_c = 2\int_{-1}^{-\infty}[(F-\tau L)F/2]'\langle\widetilde{X^2}\widetilde{X^2}\rangle d\psi, \tag{95}$$

where $' \equiv d/d\psi$.

The above system of equations possesses a rather obvious solution, i.e.,

$$v = -\tau \tag{96}$$

and

$$V_0 = F = 0. \tag{97}$$

This solution corresponds to an island that propagates with the local equilibrium ion fluid. Moreover, the fact that $V_0 = F = 0$ implies that the ion poloidal and toroidal velocity profiles are both *fully relaxed* to their neoclassical values in the vicinity of the island [see Eqs. (69) and (70)]. The (normalized) island phase velocity in the laboratory frame takes the value

$$\hat{V}_p = \hat{V}_{EB} + v = \hat{V}_{\rm nc}. \tag{98}$$

In other words, the relaxation of the poloidal and toroidal velocity profiles to their neoclassical values, under the action of poloidal and toroidal flow damping, forces the island phase velocity V_p to take the fixed value $V_{\rm nc}$, which is completely determined from neoclassical theory. It follows from Eqs. (95) and (97) that $J_c=0$, i.e., the ion polarization term in the Rutherford equation is zero. We conclude that an *isolated* magnetic island lying in the intermediate damping regime is forced to propagate with the local equilibrium ion fluid, has a fixed phase velocity (in the laboratory frame) determined from neoclassical theory, and experiences no stabilizing effect due to the ion polarization current. Of course, this conclusion is completely consistent with the results of Sec. IV B, where it was demonstrated that, even in the weak/intermediate damping regime, a sufficiently high level of flow damping leads to an island solution characterized by $v=-\tau$ and $J_c=0$.

Suppose, however, that the island is locked, e.g., suppose a resonant error field exerts an electromagnetic locking force on the island which is sufficiently large to ensure that the island phase velocity in the laboratory frame V_p is zero. In this case, the phase velocity parameter v is no longer set by Eq. (37) since the island is subject to a nonzero electromagnetic locking force [which can be calculated from Eq. (36)]. Instead, v is determined by the requirement $\hat{V}_p=\hat{V}_{EB}+v=0$. It immediately follows that

$$v = -\hat{V}_{EB} = -\tau - \hat{V}_{\rm nc}. \tag{99}$$

In this case, if $\hat{V}_{\rm nc}\neq 0$, then the solution to Eq. (92) becomes nontrivial. In fact, we find that

$$\xi V_0 = \left[\frac{\hat{\nu}_\theta(\epsilon/q)^2}{\hat{\nu}_\theta(\epsilon/q)^2+\hat{\nu}_\phi}\right]\hat{V}_{\rm nc} \tag{100}$$

inside the separatrix, whereas

$$\xi V_0 = -F\langle X^2\rangle + \hat{V}_{\rm nc} \tag{101}$$

and

$$0 = \frac{d}{d\psi}\left[\langle X^2\rangle\frac{d}{d\psi}(\langle X^2\rangle F)\right] - \frac{\hat{\nu}_\theta}{\hat{\mu}}\left(\frac{\epsilon}{q}\right)^2 F[\langle X^2\rangle\langle 1\rangle - 1] - \frac{\hat{\nu}_\phi}{\hat{\mu}}[F\langle X^2\rangle - \hat{V}_{\rm nc}]\langle 1\rangle \tag{102}$$

outside the separatrix. The boundary conditions are

$$F(\psi=-1) = \frac{\pi}{4}\left[\frac{\hat{\nu}_\phi}{\hat{\nu}_\theta(\epsilon/q)^2+\hat{\nu}_\phi}\right]\hat{V}_{\rm nc} \tag{103}$$

just outside the separatrix and

$$F(\psi\to-\infty) = \frac{\hat{V}_{\rm nc}}{\sqrt{-2\psi}} \tag{104}$$

a long way from the separatrix. Thus, if the so-called *neoclassical island phase velocity*,

$$V_{\rm nc} = V_{\theta i}^{\rm nc} - (\epsilon/q)V_{\varphi i}^{\rm nc}, \tag{105}$$

is nonzero, then the poloidal and toroidal ion velocity profiles cannot fully relaxed to their neoclassical values in the vicinity of a locked island, and the ion polarization parameter J_c, specified in Eq. (95), is consequently *nonzero*. We conclude that, whereas an isolated island in the intermediate damping regime does not have an ion polarization term in its Rutherford equation, a comparable locked island does have such a term.

B. Numerical results

Figures 7–10 show the ion polarization parameter J_c and the *locking force parameter*, $\hat{J}_s=J_s/\hat{\nu}_\theta$ [see Eq. (36)], calculated as functions of the *neoclassical velocity parameter*,

$$U_{\rm nc} = \left[\frac{\hat{\nu}_\phi}{\hat{\nu}_\theta(\epsilon/q)^2+\hat{\nu}_\phi}\right]\hat{V}_{\rm nc} \tag{106}$$

for a locked island in the intermediate damping regime. The calculations are performed for a range of different values of the *poloidal damping parameter* $(\hat{\nu}_\theta/\hat{\mu})(\epsilon/q)^2$ and the *toroidal damping parameter*, $\hat{\nu}_\phi/\hat{\mu}$. The details of the calculation are given in Appendix D.

It can be seen from the figures that $\hat{J}_s\propto U_{\rm nc}$ over a wide range of parameter values. In particular, $\hat{J}_s=0$ when $U_{\rm nc}=0$, i.e., no locking force is needed to lock a magnetic island whose neoclassical phase velocity $V_{\rm nc}$ is zero. On the other hand, if $V_{\rm nc}>0$—i.e., if the neoclassical island phase velocity is in the *electron diamagnetic direction*—then $\mathrm{Im}(\Delta' w)$

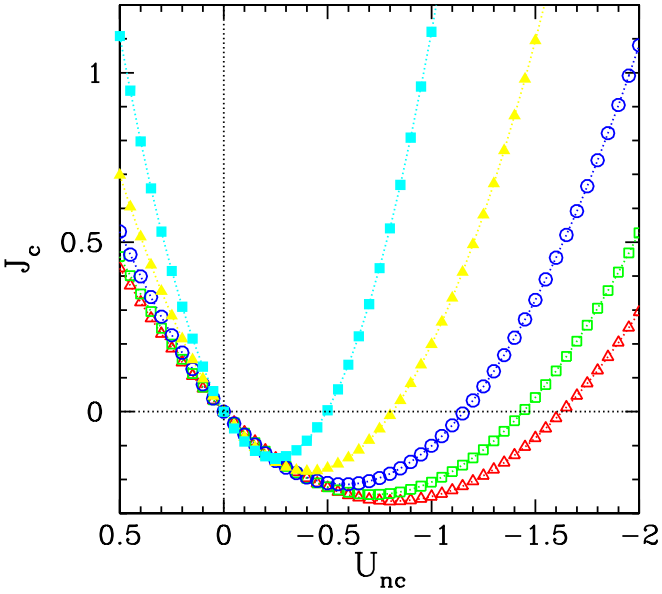

FIG. 7. (Color online) The ion polarization parameter J_c calculated as a function of the neoclassical velocity parameter U_{nc} for a locked island in the intermediate damping regime with various values of the poloidal damping parameter $(\hat{\nu}_\theta/\hat{\mu})(\epsilon/q)^2$. The red (open triangle), green (open square), blue (open circle), yellow (solid triangle), and cyan (solid square) curves correspond to $(\hat{\nu}_\theta/\hat{\mu})(\epsilon/q)^2=0.25$, 0.5, 1, 2, and 4, respectively. The values of the other parameters used in the calculations are $\tau=1$, $\hat{\nu}_\phi/\hat{\mu}=1$, and $\delta_s=10^{-6}$.

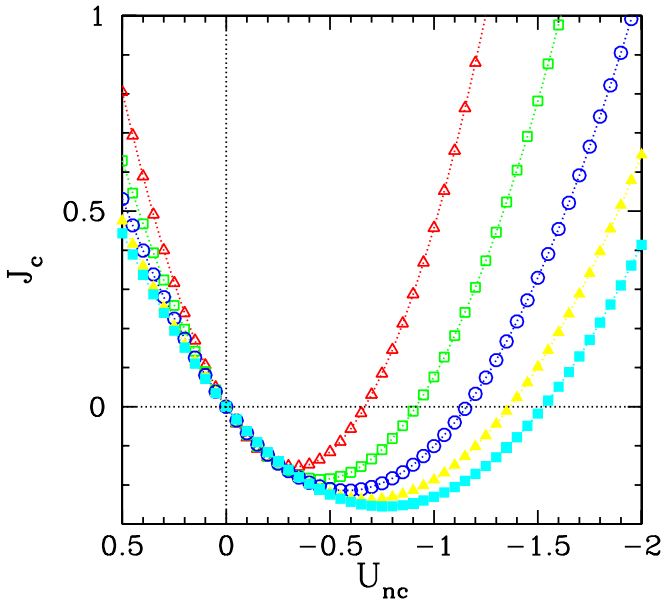

FIG. 9. (Color online) The ion polarization parameter J_c calculated as a function of the neoclassical velocity parameter U_{nc} for a locked island in the intermediate damping regime, with various values of the toroidal damping parameter, $\hat{\nu}_\phi/\hat{\mu}$. The red (open triangle), green (open square), blue (open circle), yellow (solid triangle), and cyan (solid square) curves correspond to $\hat{\nu}_\phi/\hat{\mu}=0.25$, 0.5, 1, 2, and 4, respectively. The values of the other parameters used in the calculations are $\tau=1$, $(\hat{\nu}_\theta/\hat{\mu})(\epsilon/q)^2=1$, and $\delta_s=10^{-6}$.

>0—i.e., the island experiences an electromagnetic locking force due to the error field which acts in the *ion diamagnetic direction*—and vice versa.

It can also be seen from the figures that $J_c>0$ whenever $V_{nc}>0$. In other words, a locked island in the intermediate damping regime experiences a *destabilizing* effect from the ion polarization current if its neoclassical phase velocity is in the *electron diamagnetic direction*. Of course, $J_c=0$ when $V_{nc}=0$—i.e., there is no polarization effect if the neoclassical island phase velocity is zero. Finally, if $V_{nc}<0$ then $J_c<0$ for small to moderate values of $|V_{nc}|$, and $J_c>0$ for large values of $|V_{nc}|$. In other words, a locked island in the intermediate damping regime experiences a *stabilizing* effect

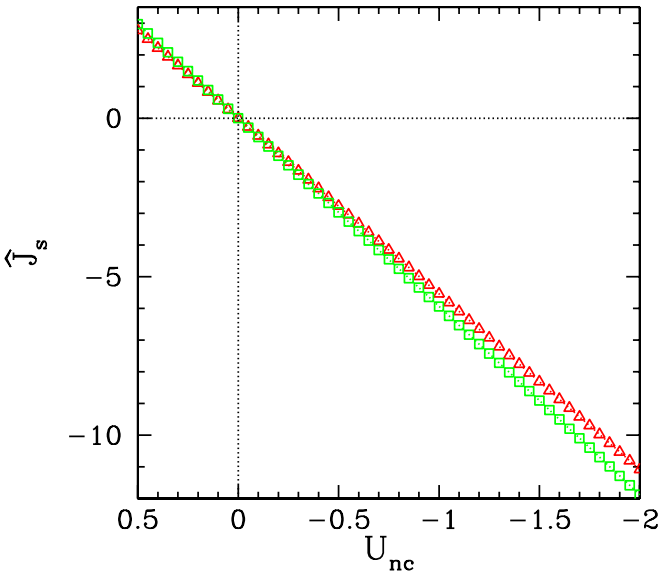

FIG. 8. (Color online) The locking force parameter $\hat{J}_s$ calculated as a function of the neoclassical velocity parameter U_{nc} for a locked island in the intermediate damping regime with various values of the poloidal damping parameter $(\hat{\nu}_\theta/\hat{\mu})(\epsilon/q)^2$. The red (open triangle) and green (open square) curves correspond to $(\hat{\nu}_\theta/\hat{\mu})(\epsilon/q)^2=0.25$ and 4, respectively. The values of the other parameters used in the calculations are $\tau=1$, $\hat{\nu}_\phi/\hat{\mu}=1$, and $\delta_s=10^{-6}$.

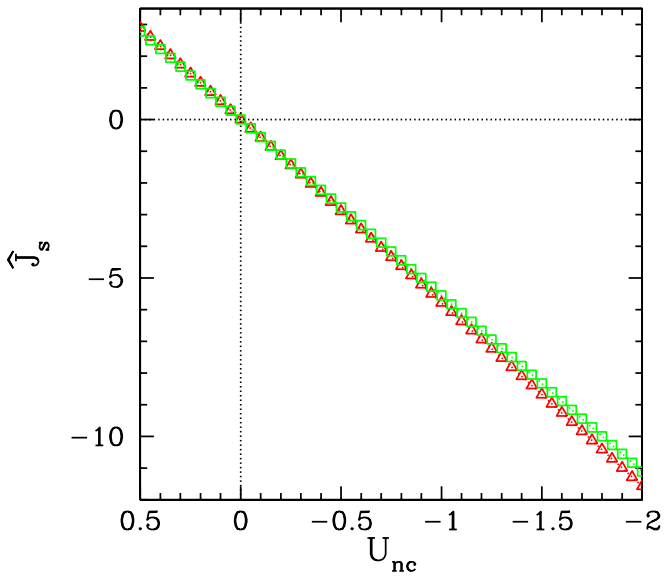

FIG. 10. (Color online) The locking force parameter $\hat{J}_s$ calculated as a function of the neoclassical velocity parameter U_{nc} for a locked island in the intermediate damping regime with various values of the toroidal damping parameter, $\hat{\nu}_\phi/\hat{\mu}$. The red (open triangle) and green (open square) curves correspond to $\hat{\nu}_\phi/\hat{\mu}=0.25$ and 4, respectively. The values of the other parameters used in the calculations are $\tau=1$, $(\hat{\nu}_\theta/\hat{\mu})(\epsilon/q)^2=1$, and $\delta_s=10^{-6}$.

from the ion polarization current if its neoclassical phase velocity is in the ion diamagnetic direction, and the magnitude of the velocity is not too large; otherwise, it experiences a *destabilizing* effect.

Now, according to standard neoclassical theory[12,19–21]

$$V_{\theta i}^{\rm nc} = K_{\theta i}\tau\eta_i V_{*e}, \tag{107}$$

$$V_{\phi i}^{\rm nc} = -K_{\phi i}\tau\eta_i V_{*e}\frac{q}{\epsilon}, \tag{108}$$

where $\eta_i = L_n/L_{Ti}$, L_{Ti} is the *ion temperature gradient scale length*, and $K_{\theta i}$ and $K_{\phi i}$ are $\mathcal{O}(1)$ dimensionless parameters that depend primarily on collisionality. Note that $\eta_i > 0$ in a conventional tokamak plasma equilibrium. Furthermore, $K_{\theta i}$ and $K_{\phi i}$ are both *positive* in a collisional plasma. It follows that

$$\hat{V}_{\rm nc} = (K_{\theta i} + K_{\phi i})\tau\eta_i \tag{109}$$

is also *positive*, i.e., that the neoclassical island phase velocity is in the electron diamagnetic direction. Hence, we conclude that a locked magnetic island in the intermediate damping regime experiences a destabilizing effect from the ion polarization current when embedded in a collisional tokamak plasma equilibrium with conventional profiles. Note that a comparable isolated (i.e., rotating) island embedded in the same plasma would experience *no effect* from the polarization current. This phenomenon may offer an explanation for the experimental observation that locked magnetic islands in tokamak plasmas generally seem to be much more unstable than comparable rotating islands (even in situations in which the loss of wall stabilization is a small effect), and that locked magnetic islands driven by resonant error fields in otherwise tearing stable plasmas tend to be *strongly amplified* by the plasma (even at low-β).[32]

VI. SUMMARY

Starting from a drift-MHD fluid model of plasma dynamics which contains phenomenological parallel and perpendicular ion viscosity operators (see Sec. II C) and using a single-helicity approximation (see Sec. II D), we derived a closed set of reduced neoclassical-MHD equations which are suitable for investigating the dynamics of a helical magnetic island in a standard large aspect-ratio low-β circular cross-section tokamak plasma equilibrium (see Sec. II E). In addition to conventional resistive-MHD effects, these equations incorporate electron and ion diamagnetism (including the contribution of the ion gyroviscous tensor), poloidal and toroidal flow damping, cross flux-surface momentum and particle transport, the sound wave, and the drift wave. The equations neglect the compressible Alfvén wave, electron inertia, the electron viscosity tensor (and, hence, the bootstrap current), magnetic field-line curvature, and finite ion orbit widths.

Using the aforementioned reduced neoclassical-MHD equations, we have developed a theory of magnetic island dynamics which is optimized for islands of width $w \sim \epsilon^{-1}\rho_i \gg \rho_s$, where $\epsilon \ll 1$ is the inverse aspect ratio of the plasma, ρ_i is the ion gyroradius, and ρ_s is the ion sound gyroradius.

The main aims of our analysis are the prediction of the island *phase velocity*, relative to the plasma, as well as the magnitude and sign of the *ion polarization term* appearing in the island's Rutherford equation. The phase velocity is determined by a *force balance constraint* which is derived directly from the parallel ion vorticity equation (see Sec. II J). According to this constraint, the net electromagnetic force acting on the island region must balance the net flow damping force acting in the same direction, i.e., the diamagnetic direction. Of course, for an isolated magnetic island which is not interacting electromagnetically with any external structures, such as a resistive wall or a resonant error field, the net electromagnetic force is zero. Hence, the phase velocity of such an island is determined by the constraint that there be *zero net damping force acting on the island region* in the diamagnetic direction. It can be demonstrated that this criterion is fully consistent with the criterion previously used in Ref. 10 to determine the phase velocity of an isolated magnetic island in the absence of flow damping, i.e., that there be zero net ion viscous force acting on the island region in the diamagnetic direction (see Sec. IV B 2). Once the island phase velocity has been determined, the calculation of the polarization term in the Rutherford equation is relatively straightforward (see subsection ofSecIII).

Our analysis is based on the assumptions that $\nu_\theta \ll \omega_{*e}$ and $\nu_\varphi \sim (\epsilon/q)^2\nu_\theta$, where ν_θ is the poloidal flow damping rate, ν_φ is the poloidal flow damping rate, ω_{*e} is the electron diamagnetic frequency, and q is the safety factor at the island rational surface. The former assumption is only likely to be valid in a large aspect-ratio collisional tokamak plasma equilibrium (see Sec. II F). Given these assumptions, we can identify *four* distinct flow damping regimes. In the *negligible damping regime*, $\nu_\theta \ll \mu/(n_0 m_i w^2)$, where μ is the ion perpendicular viscosity, n_0 is the electron number density, and m_i is the ion mass. In the weak damping regime, $\nu_\theta \sim \mu/(n_0 m_i w^2)$. In the weak/intermediate damping regime, $\nu_\theta \sim \mu/(n_0 m_i \rho_s^2)$. Finally, in the intermediate damping regime, $\omega_{*e} \gg \nu_\theta \gg \mu/(n_0 m_i \rho_s^2)$. (The so-called *strong damping regime*, in which $\nu_\theta \gtrsim \omega_{*e}$, is not investigated in this paper.)

In the negligible damping regime (see Sec. IV B 2), the dominant physical effect is a *resonant interaction* between the ion flow in the vicinity of the island and the sound wave. This interaction is strongest when $w \sim \rho_s(L_s/L_n)$, where L_s is the magnetic shear length and L_n is the density gradient scale length. If $w \gg \rho_s(L_s/L_n)$, then an isolated island propagates with the local equilibrium ion fluid, and the polarization term in its Rutherford equation is small and stabilizing. If $\rho_s \ll w \ll \rho_s(L_s/L_n)$, then the island propagates with the local equilibrium guiding center fluid, and the polarization term is again small and stabilizing. Finally, if $w \sim \rho_s(L_s/L_n)$, then the island propagates at some intermediate velocity, and the polarization term is large and stabilizing. The dominant contribution to the polarization term comes from a *boundary layer* of thickness $\rho_s \ll w$ located on the island separatrix. Furthermore, calculations which neglect the finite thickness of this layer tend to overestimate the magnitude of the polarization term.

In the weak damping regime (see Sec. IV B 3), poloidal flow damping is able to force an isolated island to propagate

with the local equilibrium ion fluid by relaxing the sheared ion flow in the region outside the separatrix to its neoclassical profile. However, the damping is not strong enough to relax the sheared flow in the separatrix boundary layer. Hence, the contribution of this layer to the ion polarization term in the Rutherford equation persists, and the polarization term is consequently similar to that obtained in the negligible damping regime.

In the weak/intermediate damping regime (see Sec. IV B 4), poloidal flow damping is strong enough to relax the sheared ion flow in the separatrix layer, and the contribution of the layer to the ion polarization term in the Rutherford equation is greatly reduced. Hence, the polarization term is much smaller than that obtained in the negligible damping regime, and approaches zero as the damping rate increases.

Finally, in the intermediate damping regime (see Sec. V), flow damping is sufficiently strong to completely relax the ion poloidal and toroidal velocity profiles in the vicinity of an isolated island to their neoclassical profiles. Consequently, such an island is forced to propagate with the local equilibrium ion fluid, has a fixed phase velocity (in the laboratory frame) which is determined from neoclassical theory—this velocity is of order the diamagnetic velocity, and is in the electron diamagnetic direction (at least, in a collisional plasma)—and has no ion polarization term in its Rutherford equation. On the other hand, if the island is locked to a resonant error field (so that its phase velocity is zero), then the ion flow in the vicinity of the island is unable to fully relax since the island phase velocity (in the laboratory frame) is forced away from its preferred neoclassical value (which is generally nonzero), and a polarization term consequently appears in the Rutherford equation. Moreover, this term is destabilizing (assuming that the neoclassical island phase velocity is in the electron diamagnetic direction). Hence, in the intermediate damping regime, a locked island is subject to a destabilizing ion polarization effect to which a comparable rotating island is not subject. We speculate that this phenomenon may offer an explanation for the experimentally observed anomalous instability of locked magnetic islands in tokamak plasmas.

Probably, the most unsatisfactory aspect of the analysis presented in this paper is the treatment of the separatrix boundary layer. This treatment is problematic because, strictly speaking, our secondary expansion (42)–(44) breaks down on length scales below ρ_s, which is the characteristic thickness of the layer. Moreover, the fluid approach taken throughout this paper becomes invalid, due to finite ion gyroradius effects, on length scales below $\rho_i=\sqrt{\tau}\rho_s$. Hence, if $\tau\gtrsim 1$, then the fluid approach is questionable in the separatrix layer. Fortunately, the overall island solution does not exhibit a strong dependence on the exact details of the separatrix layer solution. Another problem is that a more careful treatment of the separatrix layer, such as that described Ref. 33, indicates that, under certain circumstances, such a layer can emit *drift-acoustic waves*. According to Ref. 33, this effect, which is missing from our treatment of the layer, generally only has a significant influence on the overall island solution when the island propagates in the *electron* diamagnetic direction. Fortunately, this is not the case for the island solutions described in this paper, which all propagate in the *ion* diamagnetic direction. In summary, there are good reasons for supposing that the treatment of the separatrix layer presented in this paper is, at least, adequate. Clearly, however, more research needs to be done on the exact details of the separatrix layer before we can be absolutely certain of this.

ACKNOWLEDGMENTS

This research was funded by the U.S. Department of Energy under Contract No. DE-FG05-96ER-54346.

APPENDIX A: FLUX-SURFACE FUNCTIONS

It is helpful to define the flux-surface label $k=\sqrt{(1-\psi)/2}$. It follows that $k=0$ at the island O-point, $k=1$ at the X-point/separatrix, and $k\to\infty$ as $|X|\to\infty$. It is also helpful to define the complete elliptic integrals

$$E(l)=\int_0^{\pi/2}(1-l^2\sin^2\varphi)^{1/2}d\varphi, \tag{A1}$$

$$K(l)=\int_0^{\pi/2}(1-l^2\sin^2\varphi)^{-1/2}d\varphi. \tag{A2}$$

It is easily demonstrated that $E(0)=K(0)=\pi/2$, $E(1)=1$, and $K(l)\to\ln 4-(1/2)\ln(1-l^2)$ as $l\to 1$. Furthermore,

$$\langle 1\rangle=\begin{cases}K(k)/\pi, & k<1\\ K(1/k)/k\pi, & k\geq 1,\end{cases} \tag{A3}$$

$$\langle X^2\rangle=(4/\pi)kE(1/k),\quad k\geq 1, \tag{A4}$$

$$\langle X^4\rangle=(16/3\pi)k^3[2(2-1/k^2)E(1/k)-(1-1/k^2)\times K(1/k)],\quad k\geq 1. \tag{A5}$$

APPENDIX B: ISOLATED ISLAND IN WEAK DAMPING REGIME

The discontinuity in the profile function $L(k)$ (see Appendix A) across the island separatrix ($k=1$)—recall that $L=0$ just inside the separatrix, while $L=-\pi/4$ just outside—arises from the change in topology of the magnetic flux surfaces across the separatrix, combined with the fact that the ion and electron fluids are both tied to magnetic field lines. However, as is well known, in highly magnetized plasma the ion fluid ceases to be tied to magnetic field lines on length scales below the ion sound gyroradius ρ_s. Hence, we would expect the discontinuity in $L(k)$ to be resolved on the ρ_s scale (i.e., the ρ scale in normalized units). It follows that in the immediate vicinity of the separatrix we can regularize the discontinuity by writing[34,35]

$$L(y)\simeq-\frac{\pi}{4}(1-e^{-y}) \tag{B1}$$

for $y\geq 0$, where $y=(k-1)/\delta_s$ and $\delta_s\sim\rho\ll 1$. To lowest order in δ_s, Eq. (76) reduces to

$$0=\frac{d}{dy}\left[A(y)(M'+\tau L')+\frac{D}{\hat{\mu}}B(y)\left(\frac{M}{M(L-M)+\alpha^2}\right)\frac{\tau}{2}\times(L-M)L'\right]-\frac{D}{\hat{\mu}}B(y)\left(\frac{M}{M(L-M)+\alpha^2}\right)\times[M'+(\tau/2)(L'+M')]L', \tag{B2}$$

where $'\equiv d/dy$, and

$$A(y)=\frac{8}{3\pi}+\mathcal{O}(\delta_s), \tag{B3}$$

$$B(y)=\frac{8}{3\pi}-\frac{4}{\pi}\frac{1}{K([1+\delta_s y]^{-1})}+\mathcal{O}(\delta_s). \tag{B4}$$

The boundary conditions are

$$M(y=0)=0, \tag{B5}$$

$$M'(y\to\infty)=0. \tag{B6}$$

Equations (B1)–(B6) can be solved to give the profile function $M(y)$ within the separatrix layer (i.e., the region $y\geq 0$), as well as the parameter

$$m\equiv M(y\to\infty). \tag{B7}$$

Note that our treatment of the separatrix layer only retains a logarithmic dependence on the layer thickness parameter δ_s and is insensitive to the exact form of the resolving function $L(y)$. Note, further, that we are neglecting any emission of drift-acoustic waves from the separatrix layer (see Ref. 33 for a discussion of this phenomenon).

Outside the separatrix layer (i.e., the region $k>1$), Eq. (76) reduces to

$$0=\frac{d}{dk}\left[A(k)(M'+\tau L')+\frac{D}{\hat{\mu}}B(k)\left(\frac{M}{M(L-M)+\alpha^2}\right)\frac{\tau}{2}\times(L-M)L'\right]-\frac{D}{\hat{\mu}}B(k)\left(\frac{M}{M(L-M)+\alpha^2}\right)[M'+(\tau/2)\times(L'+M')]L'-\frac{\hat{\nu}_\theta}{\hat{\mu}}4k[C(k)(M+\tau L)+v+\tau], \tag{B8}$$

where $'\equiv d/dk$,

$$A(k)=\frac{\langle X^4\rangle}{4k}, \tag{B9}$$

$$B(k)=\frac{\langle\widetilde{X^2}\widetilde{X^2}\rangle}{4k}=\frac{\langle X^4\rangle-\langle X^2\rangle^2/\langle 1\rangle}{4k}, \tag{B10}$$

$$C(k)=\langle X^2\rangle=\frac{4}{\pi}kE(1/k), \tag{B11}$$

$$L(k)=-(\pi/4)/[kE(1/k)] \tag{B12}$$

(see Appendix A). It is readily shown that $A(1)=8/3\pi$, $B(1+\delta)=8/3\pi+(\pi/4)/\ln[(1+\delta)^{-1}]$, $C(1)=4/\pi$, $L(1)=-\pi/4$; plus $A(k)\to 2k^2$, $B(k)\to 1/4k^2$, $C(k)\to 2k$, $L(k)\to -1/2k$ as $k\to\infty$. Here, $0<\delta\ll 1$. The boundary conditions are

$$M(k=1)=m, \tag{B13}$$

$$M(k\to\infty)=-v/(2k), \tag{B14}$$

where m is determined from the separatrix layer solution [see Eq. (B7)]. Equation (B8) can be solved, subject to the above two boundary conditions, to give the profile function $M(k)$ in the region $k>1$. Incidentally, m represents the value of the profile function $M(k)$ immediately outside the separatrix layer. Of course, $M(k)=0$ everywhere inside the separatrix. It follows that the profile function $M(k)$ is *discontinuous* across the island separatrix. Note, however, that this discontinuity is entirely driven by the corresponding discontinuity in the profile function $L(k)$. Moreover, the discontinuity in $M(k)$ is also resolved on the ρ_s length scale within the separatrix layer.

The island phase velocity parameter v is determined from the force balance constraint (79), which reduces to

$$0=(v+\tau)\int_0^1 D(k)dk+\int_1^\infty\{4k[M(k)+\tau L(k)]+D(k)(\nu+\tau)\}dk, \tag{B15}$$

where

$$D(k)=4k\langle 1\rangle=\begin{cases}4kK(k)/\pi, & k<1\\ 4K(1/k)/\pi, & k\geq 1\end{cases} \tag{B16}$$

(see Appendix A). The contribution of the separatrix layer to the force balance constraint is negligible.

The ion polarization parameter, J_c, is given by Eq. (81), which reduces to

$$J_c=\int_1^\infty 4B(y)\left\{\frac{dM}{dy}[M(y)+\tau L(y)]+M(y)\left(\frac{dM}{dy}+\tau\frac{dL}{dy}\right)\right\}dy+\int_1^\infty 4kB(k)\times\left\{\frac{dM}{dk}[M(k)+\tau L(k)]+M(k)\left(\frac{dM}{dk}+\tau\frac{dL}{dk}\right)\right\}dk, \tag{B17}$$

where the first term on the right-hand side represents the contribution of the separatrix layer to the ion polarization parameter, whereas the second term represents the contribution from the region beyond the separatrix.

APPENDIX C: ISOLATED ISLAND IN WEAK/INTERMEDIATE DAMPING REGIME

In the limit in which the weak damping parameter, $\hat{\nu}_\theta/\hat{\mu}$, is very much larger than unity, the poloidal ion flow in the region outside the separatrix relaxes to its neoclassical value everywhere apart from a thin region located just outside the separatrix of thickness (in k) $\sim\sqrt{\hat{\mu}/\hat{\nu}_\theta}$. Thus, beyond this region, we have

$$L(k)=-(\pi/4)/[kE(1/k)], \tag{C1}$$

$$M(k)=vL(k) \tag{C2}$$

(see Appendix A).

In the immediate vicinity of the separatrix, we can again write

$$L(y) \simeq -\frac{\pi}{4}(1-e^{-y}) \tag{C3}$$

for $y \geq 0$, where $y=(k-1)/\delta_s$ and $\delta_s \sim \rho \ll 1$. To lowest order in δ_s, Eq. (76) reduces to

$$0 = \frac{d}{dy}\left[A(y)(M'+\tau L') + \frac{D}{\hat{\mu}}B(y)\left(\frac{M}{M(L-M)+\alpha^2}\right)\frac{\tau}{2} \times (L-M)L'\right] - \frac{D}{\hat{\mu}}B(y)\left(\frac{M}{M(L-M)+\alpha^2}\right) \times [M' + (\tau/2)(L'+M')]L' - 4\delta_s^2\frac{\hat{\nu}_\theta}{\hat{\mu}} \times [C(y)(M+\tau L) + v + \tau], \tag{C4}$$

where $' \equiv d/dy$ and

$$A(y) = \frac{8}{3\pi} + \mathcal{O}(\delta_s), \tag{C5}$$

$$B(y) = \frac{8}{3\pi} - \frac{4}{\pi}\frac{1}{K([1+\delta_s y]^{-1})} + \mathcal{O}(\delta_s), \tag{C6}$$

$$C(y) = \frac{4}{\pi} + \mathcal{O}(\delta_s). \tag{C7}$$

Note the inclusion of the flow damping term in Eq. (C4). The boundary conditions are

$$M(y=0) = 0, \tag{C8}$$

$$M(y \to \infty) = -\frac{\pi}{4}v. \tag{C9}$$

Equations (C3)–(C9) can be solved to give the profile function $M(y)$ in the immediate vicinity of the separatrix (i.e., the region $y \geq 0$).

The island phase velocity parameter, v, is determined from the force balance constraint (79), which reduces to

$$0 = 4\delta_s \int_1^\infty Y(y)dy + (v+\tau) \times \left\{\int_0^1 D(k)dk + \int_1^\infty [D(k) + 4kL(k)]dk\right\}, \tag{C10}$$

where

$$Y(y) = M(y) + \frac{\pi}{4}(v + \tau e^{-y}) \tag{C11}$$

and

$$D(k) = \begin{cases} 4kK(k)/\pi, & k < 1 \\ 4K(1/k)/\pi, & k \geq 1 \end{cases} \tag{C12}$$

(see Appendix A). The first term on the right-hand side of Eq. (C10) originates from the immediate vicinity of the separatrix, while the term originates from the region beyond the separatrix.

The ion polarization parameter J_c is given by Eq. (81), which reduces to

$$J_c = \int_1^\infty 4B(y)\left\{\frac{dM}{dy}[M(y) + \tau L(y)] + M(y)\left(\frac{dM}{dy} + \tau\frac{dL}{dy}\right)\right\}dy + v(v+\tau) \times \int_1^\infty 8kB(k)L(k)\frac{dL}{dk}dk, \tag{C13}$$

where

$$B(k) = \frac{\langle X^4\rangle - \langle X^2\rangle^2/\langle 1\rangle}{4k} \tag{C14}$$

(see Appendix A). The first term on the right-hand side of Eq. (C13) originates from the immediate vicinity of the separatrix, while the second originates from the region beyond the separatrix.

APPENDIX D: LOCKED ISLAND IN INTERMEDIATE DAMPING REGIME

Equation (102) can be written

$$0 = \frac{d}{dk}\left[A(k)\frac{d}{dk}[A(k)Y(k)]\right] - \frac{4\hat{\nu}_\theta}{\hat{\mu}}\left(\frac{\epsilon}{q}\right)^2 \times [A(k)B(k) - 1]Y(k) - \frac{4\hat{\nu}_\phi}{\hat{\mu}}B(k)[A(k)Y(k) - 1], \tag{D1}$$

where

$$Y(k) = 2kF(k)/\hat{V}_{\rm nc}, \tag{D2}$$

$$A(k) = \frac{\langle X^2\rangle}{2k} = \frac{2}{\pi}E(1/k), \tag{D3}$$

$$B(k) = 2k\langle 1\rangle = \frac{2}{\pi}K(1/k) \tag{D4}$$

(see Appendix A). The boundary conditions are

$$Y(k=1) = \frac{\pi}{2}\left[\frac{\hat{\nu}_\phi}{\hat{\nu}_\theta(\epsilon/q)^2 + \hat{\nu}_\phi}\right] \tag{D5}$$

and

$$Y(k \to \infty) = 1. \tag{D6}$$

Equation (D1) can be solved, subject to the above two boundary conditions, to give $Y(k)$ in the region $k > 1$.

The ion polarization parameter J_c is determined by Eq. (95), which reduces to

$$J_c = \int_1^\infty C(y)\left\{\left(\frac{dF}{dy} - \tau\frac{dL}{dy}\right)F(y) + [F(y) - \tau L(y)]\frac{dF}{dy}\right\}dy + \int_1^\infty C(k)\left\{\left(\frac{dF}{dk} - \tau\frac{dL}{dk}\right)F(k) + [F(k) - \tau L(k)]\frac{dF}{dk}\right\}dk, \tag{D7}$$

where

$$F(y) = \frac{\pi}{4}\left[\frac{\hat{\nu}_\phi}{\hat{\nu}_\theta(\epsilon/q)^2 + \hat{\nu}_\phi}\right]\hat{V}_{\rm nc}(1 - e^{-y}), \tag{D8}$$

$$L(y) = -\frac{\pi}{4}(1 - e^{-y}), \tag{D9}$$

$$C(y) = \frac{32}{3\pi} - \frac{16}{\pi}\frac{1}{K([1 + \delta_s y]^{-1})} + \mathcal{O}(\delta_s), \tag{D10}$$

$$F(k) = \hat{V}_{\rm nc}\frac{Y(k)}{2k}, \tag{D11}$$

$$L(k) = -(\pi/4)/[kE(1/k)], \tag{D12}$$

$$C(k) = \langle\widetilde{X^2}\widetilde{X^2}\rangle = \langle X^4\rangle - \langle X^2\rangle^2/\langle 1\rangle \tag{D13}$$

(see Appendix A). Here, we have again resolved the discontinuities in the profile functions $F(\psi)$ and $L(\psi)$ across the separatrix (recall that both these functions are zero within the separatrix) in a boundary layer of thickness $\delta_s \sim \rho \ll 1$. The first term on the right-hand side of Eq. (D7) represents the contribution to the ion polarization parameter which originates from the boundary layer, whereas the second term represents the contribution which originates from the region beyond the separatrix.

Finally, the force balance Eq. (36) gives

$$\mathrm{Im}(\Delta' w) = \delta_e \hat{\nu}_\theta \hat{J}_s, \tag{D14}$$

where

$$\hat{J}_s = \hat{V}_{\rm nc}\left(4\left[\frac{\hat{\nu}_\phi}{\hat{\nu}_\theta(\epsilon/q)^2 + \hat{\nu}_\phi}\right]\int_0^1 D(k)dk + 8\int_1^\infty [A(k)B(k) - 1]Y(k)dk\right) \tag{D15}$$

and

$$D(k) = 4k\langle 1\rangle = \frac{4}{\pi}kK(k) \tag{D16}$$

(see Appendix A). The contribution of the boundary layer to the force balance equation is negligible.

[1] J. A. Wesson, *Tokamaks*, 3rd ed. (Oxford University Press, Oxford, 2004).
[2] A. H. Boozer, Rev. Mod. Phys. **76**, 1071 (2005).
[3] J. P. Freidberg, *Ideal Magnetohydrodynamics* (Springer, Berlin, 1987).
[4] J. A. Wesson, Nucl. Fusion **18**, 87 (1978).
[5] H. P. Furth, J. Killeen, and M. N. Rosenbluth, Phys. Fluids **6**, 459 (1963).
[6] P. H. Rutherford, Phys. Fluids **16**, 1903 (1973).
[7] F. Militello and F. Porcelli, Phys. Plasmas **11**, L13 (2004).
[8] D. F. Escande and M. Ottaviani, Phys. Lett. A **323**, 278 (2004).
[9] Z. Chang and J. D. Callen, Nucl. Fusion **30**, 219 (1990).
[10] R. Fitzpatrick and F. L. Waelbroeck, Phys. Plasmas **15**, 012502 (2008).
[11] J. D. Callen, W. X. Qu, K. D. Siebert, B. A. Carreras, K. C. Shaing, and D. A. Spong, *Proceedings of the 11th International Conference on Plasma Physics and Controlled Nuclear Fusion Research*, Kyoto, 1986 (International Atomic Energy Agency, Vienna, 1987), Vol. 2, p. 157.
[12] K. Shaing, Phys. Plasmas **10**, 1443 (2003).
[13] S. V. Konovalov, A. B. Mikhailovskii, M. S. Shirokov, and V. S. Tsypin, Plasma Phys. Controlled Fusion **44**, L51 (2002).
[14] P. H. Rutherford, *Proceeding of Course and Workshop on Basic Physics Processes of Toroidal Fusion Plasmas*, Varenna, 1985 (Commission of the European Communities, Brussels, 1986), Vol. 2, p. 531.
[15] R. D. Hazeltine and J. D. Meiss, *Plasma Confinement* (Dover, New York, 2003).
[16] M. Kotschenreuther, R. D. Hazeltine, and P. J. Morrison, Phys. Fluids **28**, 294 (1985).
[17] A. I. Smolyakov, X. Garbet, and M. Ottaviani, Phys. Rev. Lett. **99**, 055002 (2007).
[18] S. E. Kruger, C. C. Hegna, and J. D. Callen, Phys. Plasmas **5**, 4169 (1998).
[19] R. D. Hazeltine, Phys. Fluids **17**, 961 (1974).
[20] Y. B. Kim, P. H. Diamond, and R. J. Groebner, Phys. Fluids B **4**, 2996 (1992).
[21] A. J. Cole, C. C. Hegna, and J. D. Callen, Phys. Plasmas **15**, 056102 (2008).
[22] R. Fitzpatrick and F. L. Waelbroeck, Phys. Plasmas **12**, 022307 (2005).
[23] A. Furuya, M. Yagi, and S.-I. Itoh, J. Phys. Soc. Jpn. **72**, 313 (2003).
[24] A. Bergmann, E. Poli, and A. G. Peeters, Phys. Plasmas **12**, 072501 (2005).
[25] S. I. Braginskii, *Reviews of Plasma Physics* (Consultants Bureau, New York, 1965), Vol. 1, p. 205.
[26] A. I. Smolyakov, Plasma Phys. Controlled Fusion **35**, 657 (1993).
[27] R. Fitzpatrick, Nucl. Fusion **33**, 1049 (1993).
[28] J. W. Connor, F. L. Waelbroeck, and H. R. Wilson, Phys. Plasmas **8**, 2835 (2001).
[29] F. L. Waelbroeck, Phys. Rev. Lett. **95**, 035002 (2005).
[30] F. L. Waelbroeck and R. Fitzpatrick, Phys. Rev. Lett. **78**, 1703 (1997).
[31] A. I. Smolyakov, A. Hirose, E. Lazzaro, G. B. Re, and J. D. Callen, Phys. Plasmas **2**, 1581 (1995).
[32] T. C. Hender, R. Fitzpatrick, A. W. Morris, P. G. Carolan, R. D. Durst, T. Edlington, J. Ferreira, S. J. Fielding, P. S. Haynes, J. Hugill, I. J. Jenkins, R. J. La Haye, B. J. Parham, D. C. Robinson, T. N. Todd, M. Valovic, and G. Vayakis, Nucl. Fusion **32**, 2091 (1992).
[33] R. Fitzpatrick and F. L. Waelbroeck, Phys. Plasmas **12**, 122511 (2005).
[34] A. B. Mikhailovskii, V. D. Pustovitov, V. S. Tsypin, and A. I. Smolyakov, Phys. Plasmas **7**, 1204 (2000).
[35] A. B. Mikhailovskii, V. D. Pustovitov, A. I. Smolyakov, and V. S. Tsypin, Phys. Plasmas **7**, 1214 (2000).